

To: Voight-Sikorsky Aircraft Div.
United Aircraft Corp.
Att: Mr. Chas. J. McCarthy

NATIONAL ADVISORY COMMITTEE FOR AERONAUTICS

THIS DOCUMENT AND EACH AND EVERY PAGE HEREIN IS HEREBY RECLASSIFIED

FROM CONFIDENTIAL TO UNCLASSIFIED
AS PER LETTER DATED 11/22/82
Refr 122

ADVANCE CONFIDENTIAL REPORT #244

VOIGHT-SIKORSKY AIRCRAFT LIBRARY

TESTS OF A HEATED LOW-DRAG AIRFOIL

By Charles W. Frick, Jr., and George B. McCullough

Ames Aeronautical Laboratory
Moffett Field, Calif.

CLASSIFIED DOCUMENT

This document contains classified information affecting the National Defense of the United States within the meaning of the Espionage Act, U.S.C. 50-31 and 32.

Unclassified - Notice Remarkd 4/17/09

United States, appropriate civilian officers and employees of the Federal Government who have a legitimate interest therein, and to United States citizens of known loyalty and discretion who of necessity must be informed thereof.

December 1942

A244

OCR- Dec. 1942

244

SR-244

NATIONAL ADVISORY COMMITTEE FOR AERONAUTICS

ADVANCE CONFIDENTIAL REPORT

TESTS OF A HEATED LOW-DRAG AIRFOIL

By Charles W. Frick, Jr., and George B. McCullough

SUMMARY

The results of an experimental investigation of an NACA 65,2-016 heated wing are presented. The test data show the following:

1. The chordwise distribution of high skin temperatures normal for heat de-icing can be obtained with negligible effect either on the drag coefficients in the low-drag Reynolds-number range or on the maximum Reynolds number at which low drag is obtained.

2. Distribution of heat along the chord resulting in high temperatures near the minimum pressure position will result in both an increase in the minimum drag coefficients and a marked reduction in the Reynolds-number range over which low drag occurs. This marked reduction of the critical Reynolds number occurs because the decrease in the stability of the laminar boundary layer promotes earlier transition to turbulent flow.

INTRODUCTION

At the request of the Materiel Command, U. S. Army Air Forces, the effect of heat on the drag of a low-drag airfoil was investigated in the 7- by 10-foot wind tunnel of the Ames Aeronautical Laboratory. The tests were made primarily to find what changes would be experienced in the minimum drag characteristics of the wing with heat de-icing, and to compare these effects with the results of tests of a low-drag wing equipped with rubber de-icing boots (reference 1).

The effects of the addition of heat to the laminar boundary layer that occur when the skin temperature is increased may be studied under the following four headings:

- (a) skin friction
- (b) boundary-layer stability
- (c) Meredith effect
- (d) critical speed

The latter two are eliminated for the purposes of the present tests because the maximum Mach number attainable in this tunnel, 0.4, is considerably below the critical value for this airfoil, and moreover is not sufficiently large to find any appreciable change in drag from Meredith effect. The results of the tests, therefore, are discussed under the first two headings only.

Nomenclature

The symbols used throughout this report are defined as follows:

- V free-stream velocity
- U local velocity just outside the boundary layer
- u local velocity in the boundary layer
- c wing chord
- x distance from the leading edge along the chord
- y distance normal to the surface
- δ boundary-layer thickness defined as the distance normal to the surface to the point in the boundary layer where u is equal to $0.707U$
- θ the momentum thickness of the boundary layer

$$\theta = \int_0^h \frac{\rho}{\rho_L} \frac{u}{U} \left(1 - \frac{u}{U}\right) dy$$

where h is large enough to enclose the entire friction layer

ν	the kinematic viscosity
μ	the absolute viscosity
ρ_o	free-stream density
ρ_L	local density outside boundary layer
ρ	local density inside boundary layer
R_c	Reynolds number based on the chord (Vc/ν)
R_δ	boundary-layer Reynolds number based on thickness, δ , ($U\delta/\nu$)
R_θ	boundary-layer Reynolds number based on momentum thickness, θ , ($U\theta/\nu$)
$R_{\delta_{crit}}$	and $R_{\theta_{crit}}$ are values of these parameters at which the laminar boundary layer becomes turbulent
$R_{c_{crit}}$	is defined as the maximum Reynolds number at which low drag occurs
t_o	free-stream air temperature, $^{\circ}F$
T_o	free-stream air temperature, $^{\circ}F$ absolute
t_L	local temperature outside the boundary layer, $^{\circ}F$
T_L	local temperature outside the boundary layer, $^{\circ}F$ absolute
t	local temperature inside the boundary layer, $^{\circ}F$
T	local temperature inside the boundary layer, $^{\circ}F$ absolute
t_e	surface temperature at any chordwise point, $^{\circ}F$
θ_e	temperature difference across the boundary layer = $(t_e - t_L)$
θ	temperature difference between any point in the boundary layer and the surface temperature, $(t_e - t)$

Description of Apparatus

Tests of a heated wing were made in the 7- by 10-foot tunnel at AAL. This tunnel is of the closed-throat, rectangular-section, single-return type, capable of air speeds of 300 miles per hour. The turbulence level of the air stream is such that a wing chord of 7 feet for the 65,2-016 section was necessary in order that the critical Reynolds number, the upper limit of the low-drag range, could be exceeded.

Description of Model

The model was a 7-foot-chord by 7-foot-span NACA 65,2-016 airfoil mounted as a vertical "through model." Ordinates are given in table I.

The model is shown mounted in the tunnel in figure 1(a). The forward portion containing heating lamps was of sheet-aluminum construction, and the trailing section of laminated wood. Construction details are shown in figure 1(b). Built into the model were 26 pressure orifices and 41 iron-constantan thermocouples. The thermocouples were in three chordwise bands on the span center line and 4 inches each side extending to 41-percent chord. The pressure orifices were connected to a multiple-tube manometer, and the leads from each thermocouple were brought out to a multi-contact selector switch which was connected to a Lewis pyrometer-potentiometer. The external surface of the heated portion was bare metal and that of the unheated wood part was painted. The entire model was made aerodynamically smooth by chordwise rubbings with successively finer grit sandpaper. All power, temperature, and pressure leads were brought out through the top of the model which was sealed closed to prevent the escape of convected heat.

Local unfairnesses of the model resulted in some minor variations in the pressure distribution, as shown in figure 2, but these were not of sufficient magnitude to induce transition to turbulence.

Method of Heating

The heated portion of the wing was divided into four compartments by spanwise bulkheads on which the heating elements, nine rows of ordinary 120-volt incandescent lamp bulbs, were mounted (fig. 1(b)). The inside surface of the aluminum skin was painted a dull black to increase the absorption of radiant heat, but all other metal surfaces were bright.

The heat input appropriate to each compartment to give a temperature difference across the boundary layer of 100° F at a Reynolds number of 13,000,000 was calculated by the method of reference 2. The size, number, and location of the bulbs within each compartment were such as to give the most nearly uniform skin temperature possible within the practical limitations of the design.

Power was supplied by a direct-current generator equipped with a remote voltage control which permitted a convenient means of adjusting the over-all applied voltage.

Other Apparatus

For measurement of the temperature distribution through the boundary layer, a temperature "mouse" consisting of six thermocouples was used. Each thermocouple was made of small-diameter copper tubing through which was led a small insulated constantan wire, as shown by the sketch of figure 3(a). Heights of the thermocouples above the wing surface were adjusted by bending the copper tubing, and were measured by means of a microscope with a scale reading in thousandths of an inch. The six individual copper leads and one common constantan lead were brought out through the wing to a selector switch. Electromotive forces were read with a Leeds and Northrup potentiometer. A cold junction immersed in a vacuum bottle of ice water was used for reference.

A velocity mouse consisting of six total-head tubes and one static tube was used for measuring the velocity boundary layer. Tube heights were adjusted and read by the same method as for the temperature mouse. Figure 3(b) is a detail view showing both mice mounted on the wing.

All drag measurements were made with a momentum rake of 48 total-head tubes spaced 1/4 inch apart connected to

an integrating manometer. Lift was determined from pressure distribution. No force-test measurements on the wind-tunnel scale were made.

Free-stream air temperatures were calculated from average readings of three resistance-type thermometers located in the return passage a short distance ahead of the entrance cone. Adiabatic expansion through the entrance cone was assumed.

Test Methods and Corrections

Drag measurements.— Simultaneous pressure distribution and momentum drag data were obtained through a range of angles of attack with the model unheated and heated. Section lift coefficients were calculated by integration of the pressure distribution. Momentum drag data were computed by an adaptation of the Jones method, including correction for compressibility. No correction was made for heating of the wake because this was found to be inappreciable for the amount of heat transfer from the model. Tunnel-wall effect was corrected by the following factors based on an unpublished theory of two-dimensional tunnel-wall corrections.

$$c_{d_0} = 0.930 c'_{d_0}$$

$$c_l = 0.838 c'_l$$

$$R_c = 1.030 R'_c$$

Since the main interest was in the effect of heat on minimum drag, most of the runs were made at the ideal angle (0°) for the full range of Reynolds numbers with the model unheated and heated. Simultaneous momentum drag and temperature-distribution data were taken for these runs.

Temperature-distribution data were computed and plotted in terms of the parameter, θ_ϵ/T_0

where

$$\theta_\epsilon = (t_\epsilon - t_L)$$

- t_e skin temperature, °F
- t_L local free-stream temperature outside the boundary layer, °F
- T_0 free-stream temperature, °F absolute

Boundary-layer measurements.— Simultaneous velocity and temperature boundary-layer profile data and chordwise temperature data were obtained with the two mice mounted on the wing 6 inches either side of midspan at the same percent chord. To offset the greater heat transfer from the surface aft of the mice with consequent reduction of skin temperature resulting from turbulence in the wake of the mice, triangular-shaped areas were covered with scotch tape. These may be seen in figure 3(b).

In order to obtain true air temperatures from indications of the temperature mouse, corrections for aerodynamic heating were applied. Eckert (reference 3) has shown that the aerodynamic heating experienced by a similar type of thermocouple in laminar flow is about $0.845\sqrt{\sigma}$, times the temperature rise which would result if the air were brought to rest adiabatically. An experimental check was obtained on this constant by exposing the thermocouple mouse to an air stream of known velocity and temperature and comparing the excess temperature of the stream with the adiabatic temperature rise. The indicated temperatures measured in the boundary layer, therefore, were corrected by obtaining the velocity in the boundary layer corresponding to the position of the thermocouple and applying the above correction.

Velocity boundary-layer data were corrected for temperature on the following basis:

$$u = u' \sqrt{T/T_L}$$

The magnitude of this correction was small, and it was not considered necessary to recorrect the temperature boundary layer using the corrected values of u .

Temperature boundary layers are plotted in the form θ/θ_e where $\theta = t_e - t$, t being the local temperature inside the boundary layer. This allowed direct comparison of the temperature and velocity boundary-layer profiles.

RESULTS AND DISCUSSION

Drag effects at the ideal angle.- The major purpose of the tests discussed herein was to determine the effect of heat on the minimum drag of the airfoil section; hence most of the results obtained are concerned with the variation of minimum drag with Reynolds number at the ideal angle of attack.

Identical tests were made with three different sections of the "laminar run" heated as follows:

1. Entire laminar run (0-percent to 52.4-percent chord) heated to θ_c of 0° , 50° , 75° and 100° F.
2. Section ahead of minimum pressure (26.3-percent to 52.4-percent chord) heated to θ_c of 0° , 50° , 75° and 100° F.
3. Nose section (0-percent to 14.6-percent chord) heated to θ_c of 0° , 50° , 75° and 100° F.

Results are presented in figures 4, 5, and 6. Figure 7 is a comparison of the effects of the three types of heating for the same value of θ_c (75° F).

Examination of the data shows that the drag coefficients for all conditions remain nearly constant at a minimum value for a certain range of Reynolds numbers and then increase more or less abruptly at some critical value of the Reynolds number. This critical value has been found to occur when transition from laminar to turbulent flow in the boundary layer moves forward through the minimum pressure position. Thus, for the low-drag range of Reynolds numbers transition is behind minimum pressure and for the high-drag range following the critical Reynolds number transition is ahead of minimum pressure.

Figures 8, 9, and 10 are typical of the chordwise temperature distributions which were obtained for the various heating conditions. It will be noted from figure 8 (laminar run heated) that when the critical Reynolds number of 8,000,000 was exceeded and transition moved forward of minimum pressure on to the heated (aluminum) portion of the wing, the high rate of heat transfer in the turbulent region prevented the desired "constant" temperatures from being

maintained. A similar effect occurred for the "region ahead of minimum pressure" heated (fig. 9). However, since this deviation by its very nature occurs only after the critical Reynolds number has been attained for any given θ_c , the drag results, insofar as the effects on the value of the critical Reynolds number are concerned, were all obtained with proper heat distributions. Beyond the critical Reynolds number it may be anticipated that somewhat greater increases in drag would have been measured, had it been possible to maintain the nominal temperature distributions.

It is important to note that the "nose-heated" condition (fig. 10) gave a temperature distribution which was very close to that which is normal for heat de-icing installations. For the purpose of comparison, a typical heat de-icing distribution (taken from reference 4) is plotted on figure 10.

A study of the drag results reveals that the major effect of heat for conditions 1 and 2 was a marked reduction in the critical Reynolds number. Figure 11 presents the variation of critical Reynolds number with increasing θ_c for the three heat conditions. The critical Reynolds number is shown to be negligibly affected by heating the nose. But for the laminar run heated to a θ_c of 75° F, there resulted a decrease in the critical Reynolds number to about 8,000,000 and for the region ahead of minimum pressure heated a corresponding decrease to about 4,000,000. This compares to a critical Reynolds number of about 11,000,000 for no heat. (It may be noted that there is a definite tendency for the reduction in critical Reynolds number to approach a limiting value with increasing temperature.) Such reductions in critical Reynolds numbers would mean a serious increase in drag for an airplane equipped with a low-drag airfoil designed to operate slightly below the critical Reynolds number with no heat. However, for the nose-heated condition which simulated normal heat de-icing temperature distributions, only minor changes in R_{crit} were measured.

The minimum drag coefficients in the range of Reynolds numbers below the critical experience negligible increases for the nose-heated condition as seen from figure 6. These increments were so small that they were within the accuracy of the experimental results. For the other heat conditions, the minimum drag increases of 0.0002 to 0.0005 cannot be

accounted for by the increased shear of the laminar region as is shown by the measured momentum thicknesses of the laminar layer which indicate an actual decrease in the surface shear up to 29-percent chord. They are most probably due to the increased shear of the turbulent boundary layer just aft of transition caused by heating near the minimum pressure position, since it is unlikely that they result from increased pressure drag.

In the high-drag range of Reynolds numbers greater than the critical, approximately one-third of the drag increase can be accounted for by the increased area subjected to turbulent flow because of the forward movement of transition. The remaining two-thirds may be attributed to the pressure drag resulting from the inability of the thickened boundary layer to develop the steep pressure recovery behind minimum pressure.

Drag effects at angles other than the ideal.- The effects of heat at angles other than the ideal are in the direction which would be anticipated by the ideal angle results. Figure 12 shows that the effects of nose heat are slight, whereas with the laminar run heated the low-drag angle-of-attack range has disappeared at a Reynolds number of 11,000,000. Figure 13 extends the comparison for nose heat and "no heat" to higher lift coefficients, at a Reynolds number of 6,600,000.

Comparison with rubber de-icer effects.- Figure 14 has been prepared from the results of tests of a rubber de-icer on a low-drag wing (reference 1). A comparison is afforded of the nose-heat results with those of the rubber de-icer. (The "compression" of the c_{d_0} vs. R_c characteristics measured in the 7- by 10-foot tunnel, resulting in lower $R_{c_{crit}}$ compared with the two-dimensional tunnel, is due to the difference in turbulence levels of the two tunnels. The slight unfairness of the test wing causing the pressure waves shown on fig. 2 probably contributed to this compression.) The figure emphasizes the fact that with rubber de-icers the low-drag advantage of the laminar-flow wing is lost, while with heat de-icing it is essentially unchanged.

Boundary-layer effects.- As stated previously, the critical Reynolds number for any low-drag airfoil occurs when the transition from laminar to turbulent flow in the boundary layer moves forward along the chord through the

chordwise position of minimum pressure. This movement of transition into the pressure region whose gradient is favorable to the preservation of laminar flow has been found to be associated with the attainment of a critical value of R_{δ} (reference 5). It is known that this value of R_{δ} is affected by air stream turbulence, surface condition, and vibration. In an effort to gain some knowledge of why this stability limit was adversely affected by heating the surface, an experimental investigation of the laminar boundary layer was made for the same heat conditions as for the drag tests.

Boundary-layer surveys were made at 40-percent chord and are presented in figures 15 through 18 for the various heat conditions at θ_c of 75° F. Figure 19 showing the variation of u/U , as measured with a mouse surface tube, with Reynolds number allows the chordwise position of transition to be determined at any Reynolds number. Other surveys were made at 29-percent chord, a position well removed from the influence of transition at the lower Reynolds numbers, for the purpose of obtaining experimental data on the relationship between the temperature and velocity boundary-layer profiles. Typical results in the form of u/U and θ/θ_c are given in figures 20 to 23, inclusive.

Figure 24 presents a comparison between the calculated variation of δ , the boundary-layer thickness, with Reynolds number and the values taken from experimentally-determined profiles at the 29-percent-chord location. From these results, it is evident that for this test model the boundary-layer thickness is not inversely proportional to the square root of Reynolds number as would be expected from theory. This difference is believed to come about because of the local reversals in the pressure gradient ahead of the 29-percent-chord position due to local unfairness of the surface. For the purposes of these tests, this disagreement does not prevent a comparison between the no-heat boundary-layer results and those obtained with the various heat conditions.

The results of figure 24 indicate a reduction of R_{δ} when heat is added to the entire laminar run, or just forward of minimum pressure. An opposite effect would be anticipated from an expected increased surface shear due to higher viscosity of the heated boundary layer. This apparently contradictory result is explained by an examination of the experimental boundary-layer profiles from which the values of δ were measured. There is a marked

change in profile with heat conditions 1 and 2, which appears near the surface of the airfoil as a decrease in the velocity gradient at the surface, as compared to the no-heat profile. This decrease in $(du/dy)_{y=0}$ is sufficient to cause the profile to develop an inflection point. The consequent redistribution of momentum through the friction layer coupled with the increased local velocity resulting from decreased density of the heated boundary layer causes the upper half of the profile to "bulge" increasing the concavity.

The distortion of the laminar friction layer is associated with the type of temperature distribution through the laminar layer. This is demonstrated by the results of figure 25 which show the measured velocity boundary layers for approximately equal values of θ_c but with different distribution of temperature through the boundary layer. The distribution associated with heating the nose has very little effect in distorting the boundary layer while the steep temperature gradient from the surface resulting from heating near minimum pressure had a marked effect. (It may be noted that the temperature distribution associated with heating the nose is very similar to that obtained by aerodynamic heating where $T \sim 1/u^2$).

It is apparent from the above discussion that δ as a measure of the boundary-layer momentum loss loses its significance. A more logical criterion for the case of the artificially heated boundary layer which is distorted (or the Blasius profile accompanied by a temperature rise due to friction) is the momentum thickness, θ , since it takes into account the variation of density through the layer and is not dependent on the profile shape. The values of θ , corresponding to profiles from which the values of δ plotted in figure 24 were taken, are given as a function of the wing Reynolds number in figure 26. These data present a truer picture of the boundary layer. The loss in momentum represented as θ is seen to be approximately the same with no heat, nose heat, and for heat at minimum pressure. The measured values of θ for the laminar run heated indicate that the shear was decreased for this heat condition. This appears to be due to the fact that the decreased velocity gradient $(du/dy)_{y=0}$ experienced with this type of heating more than offset the effect of the increased viscosity on the surface shear.

It has been found that the afore-mentioned limit of the boundary-layer stability may be expressed as a critical value of the boundary-layer Reynolds number, Ud/v , where d is some characteristic length of the boundary layer. This length has been taken in past research as δ , the point in the boundary layer where $u = 0.707U$, but δ , according to the above discussion, loses its significance for these artificially heated boundary layers. (This is true also for aerodynamically heated boundary layers.) Consequently, it is logical to substitute θ for δ in the boundary-layer Reynolds number so that it becomes $U\theta/v$, which may be designated R_θ . The value of R_θ when transition occurs may be noted as $R_{\theta \text{ crit}}$.

It then follows that the occurrence of $R_{\theta \text{ crit}}$ at minimum pressure defines the critical body Reynolds number. Assuming that a given value of $R_{\theta \text{ crit}}$ is associated with the occurrence of transition anywhere in the favorable pressure gradient, we may use the variation of θ with Reynolds number at 29-percent chord to calculate the variation of R_θ with R_c at this point and from these curves determine the values of $R_{\theta \text{ crit}}$ for the heat condition which caused transition to occur this far forward. Figure 27 presents this variation of R_θ with R_c .

It is evident that the occurrence of transition will cause the variation of R_θ with R_c to become discontinuous. The value of $R_{\theta \text{ crit}}$ then is R_θ at the point of discontinuity. Thus, it is seen that $R_{\theta \text{ crit}}$ for the laminar run heated to $\theta_c = 75^\circ \text{ F}$ is 1070 and for heat applied to minimum pressure about 1190. The Reynolds numbers at which these values occur agree fairly well with the Reynolds numbers for transition at 29-percent chord for these heat conditions taken from figure 23.

For the nose-heated and no-heat boundary layers shown on figures 18 and 15, it is found that the occurrence of transition at 40-percent chord gives a value of $R_{\theta \text{ crit}}$ of about 1600. It is therefore apparent that the stability of the distorted boundary-layer profiles for these heat conditions is much less than for the convex profiles obtained with no heat or with the nose heated.

This has been verified theoretically by Tollmien (reference 6), who has shown that laminar profiles developing inflection points are essentially less stable to small oscillations than convex profiles. This, then, affords an acceptable explanation of the powerful effects that heat conditions 1 and 2 have on the critical Reynolds number and why heating the nose has little effect.

CONCLUSIONS

The results of the drag tests of the heated NACA 65,2-016 airfoil show the following:

1. The chordwise distribution of high skin temperatures in the nose region only (as used for heat de-icing) may be obtained with negligible effect either on the drag coefficients in the low-drag Reynolds-number range or on the maximum Reynolds number at which low drag is obtained.

2. Distribution of heat along the chord resulting in high skin temperatures near the minimum pressure position will result in both an increase in the minimum drag coefficients and a marked reduction in the Reynolds-number range over which they occur.

3. The marked reduction in the critical Reynolds number caused by heat near minimum pressure is due to the fact that this type of heating gives a temperature distribution in the boundary layer which promotes an inflection point in the velocity profile. The resulting boundary layer has less stability than one with a Blasius profile.

Ames Aeronautical Laboratory,
National Advisory Committee for Aeronautics,
Moffett Field, Calif.

REFERENCES

1. von Doenhoff, A. E.: Effect of Goodrich De-Icers on Drag of Airfoil Section for Douglas XA-26 Airplane. NACA G.M.R. for Materiel Division, U. S. Army Air Corps, September 8, 1941.
2. Frick, Charles W., Jr. and McCullough, George B.: A Method for Determining the Rate of Heat Transfer from a Wing or Streamline Body. NACA A.C.R., December 1942.
3. Eckert, E.: Temperature Recording in High-Speed Gases. NACA T. M. No. 983, August 1941.
4. Rodert, Lewis A., and Clousing, Lawrence A.: A Flight Investigation of the Thermal Properties of an Exhaust Heated Wing De-Icing System on a Lockheed 12-A Airplane. NACA A.R.R., June 1941.
5. Jacobs, E. N., and von Doenhoff, A. E.: Formulas for Use in Boundary-Layer Calculations on Low- Drag Wings. NACA A.C.R., August 1941.
6. Tollmien, W.: General Instability Criterion of Laminar Velocity Distributions. NACA T. M. No. 792, April 1936.

TABLE I.- ORDINATES OF 7-FOOT-CHORD

NACA 65,2-016 AIRFOIL

x Percent chord	x (in.)	y Percent chord	y (in.)
0	0	0	0
.5	.420	1.202	1.010
.75	.630	1.423	1.195
1.25	1.050	1.796	1.509
2.5	2.100	2.507	2.106
5.0	4.200	3.543	2.976
7.5	6.300	4.316	3.625
10	8.400	4.954	4.161
15	12.600	5.958	5.005
20	16.800	6.701	5.629
25	21.000	7.252	6.092
30	25.200	7.647	6.423
35	29.400	7.888	6.626
40	33.600	7.995	6.716
45	37.800	7.938	6.668
50	42.000	7.672	6.444
55	46.200	7.180	6.031
60	50.400	6.497	5.457
65	54.600	5.647	4.743
70	58.800	4.693	3.942
75	63.000	3.742	3.143
80	67.200	2.763	2.321
85	71.400	1.797	1.509
90	75.600	.982	.825
95	79.800	.340	.286
100	84.000	0	0

*Values are based on segment of
of C.P. 100 487-11-13*

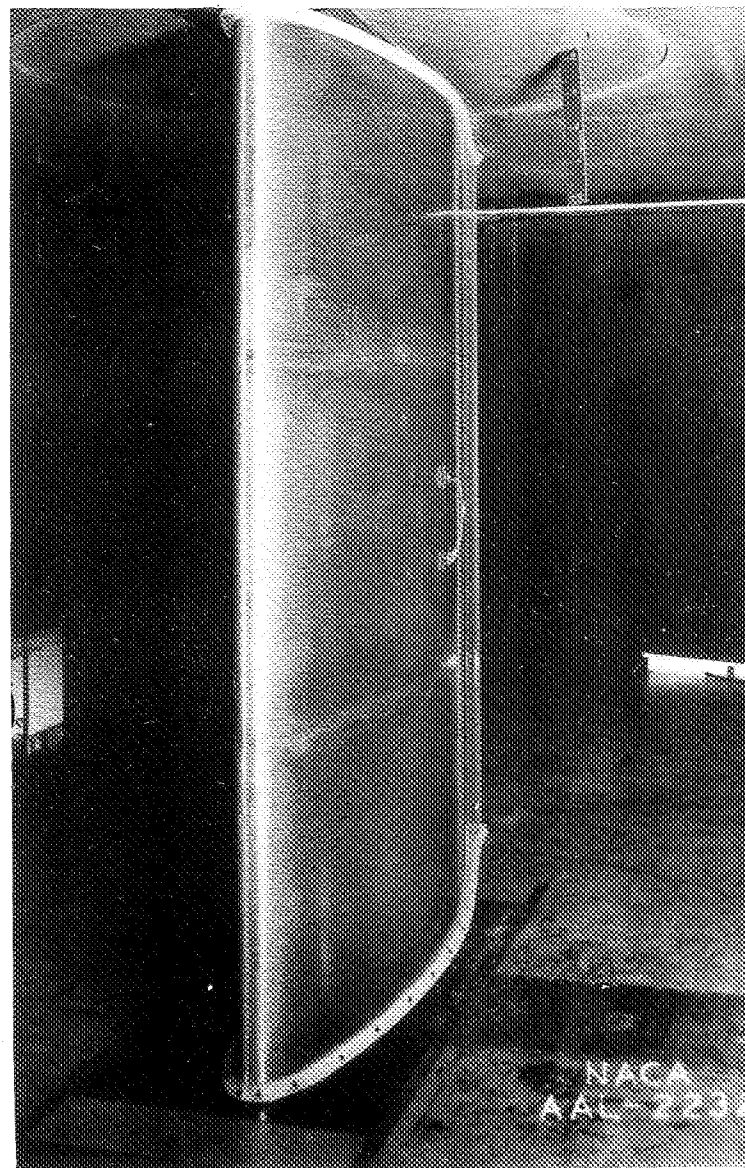
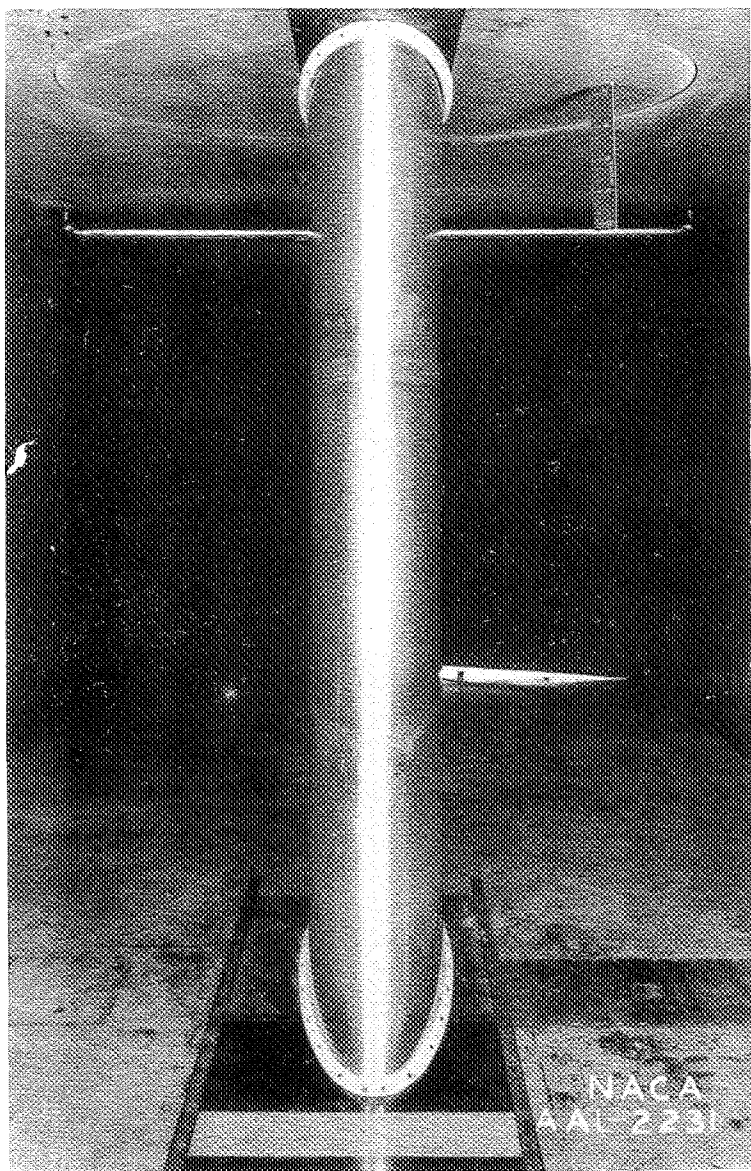


Figure 1a.- Three-quarters and front views of model mounted in tunnel.

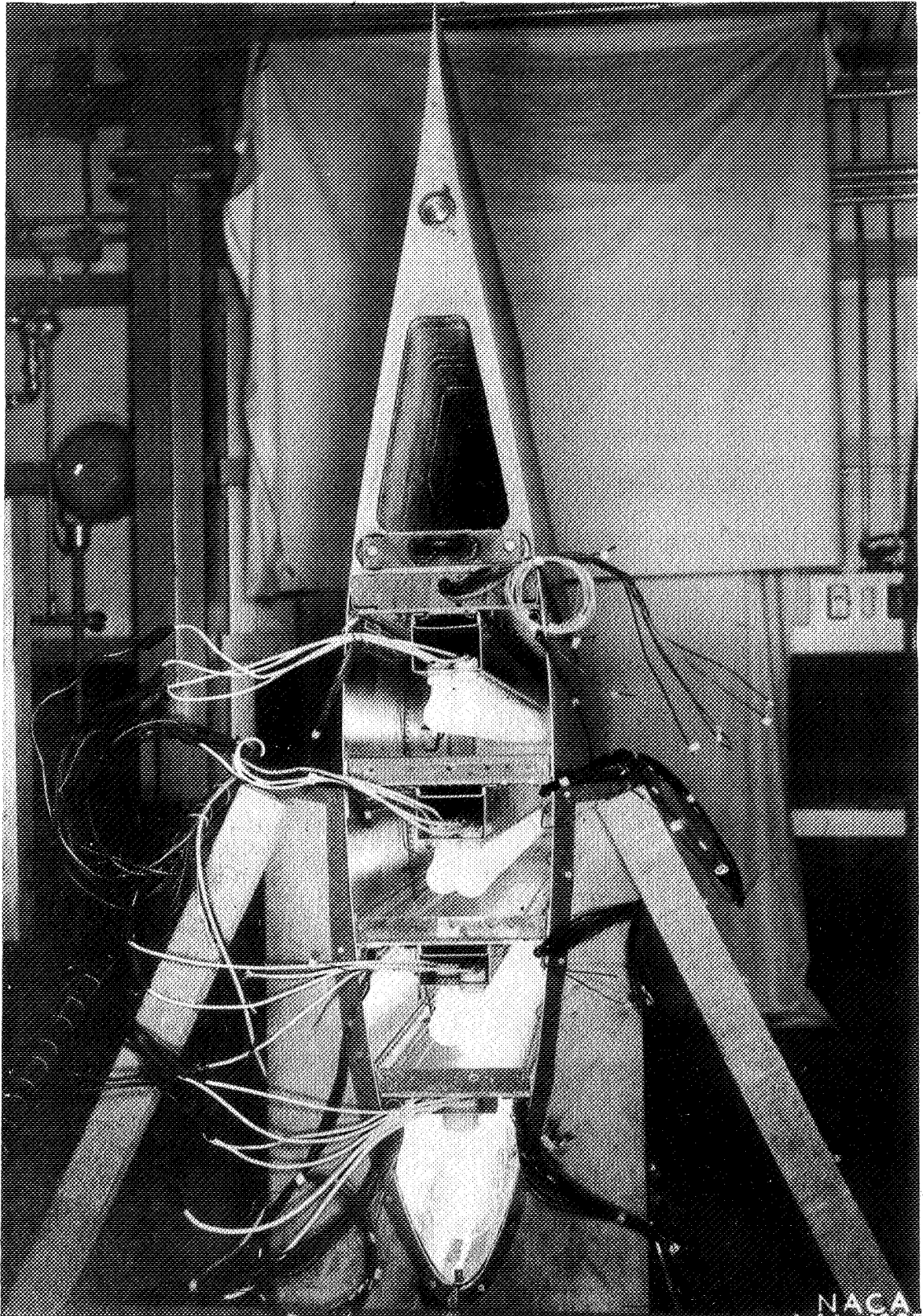


Figure 1b.- Top view of model showing heating lamps.

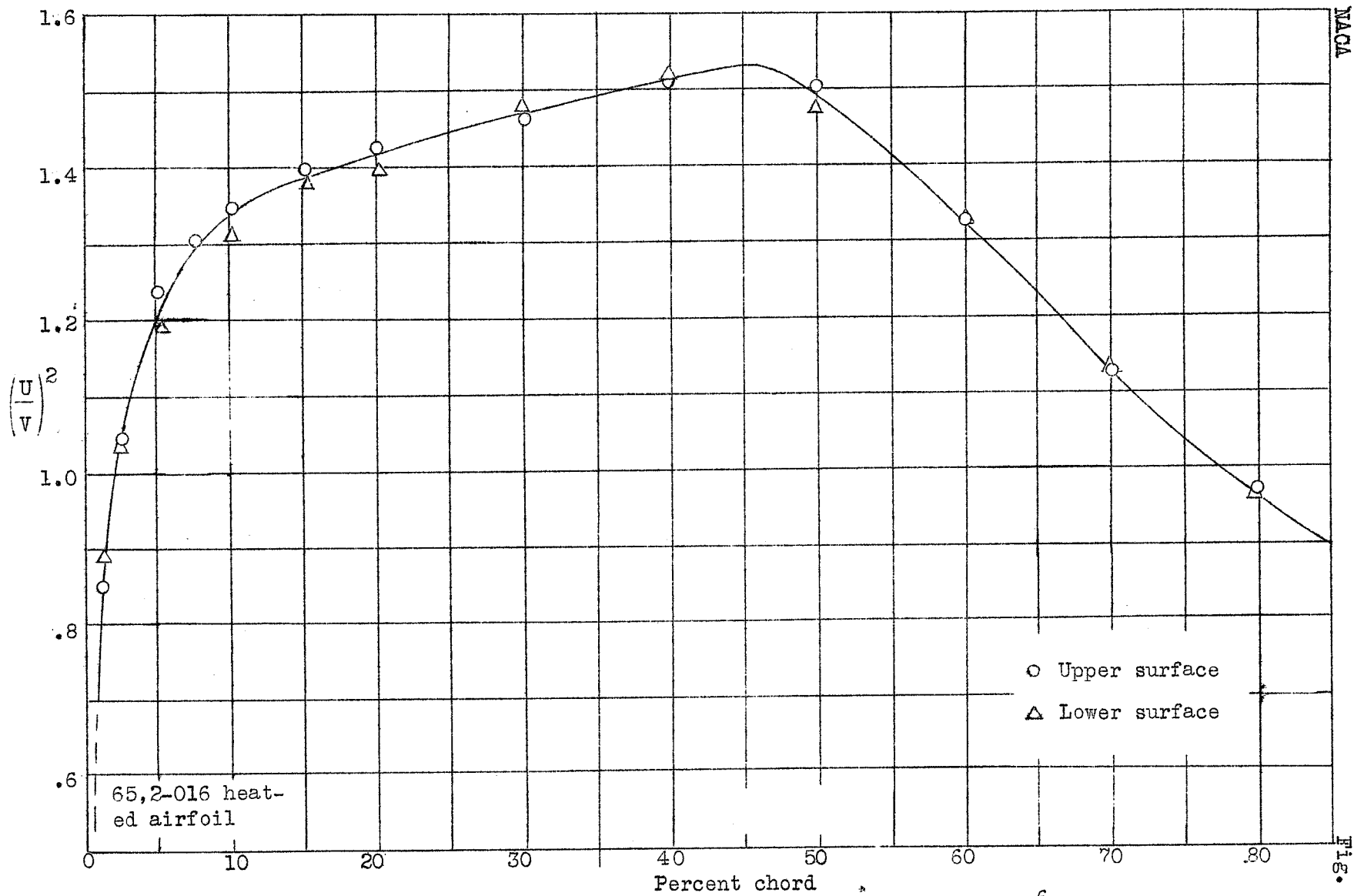
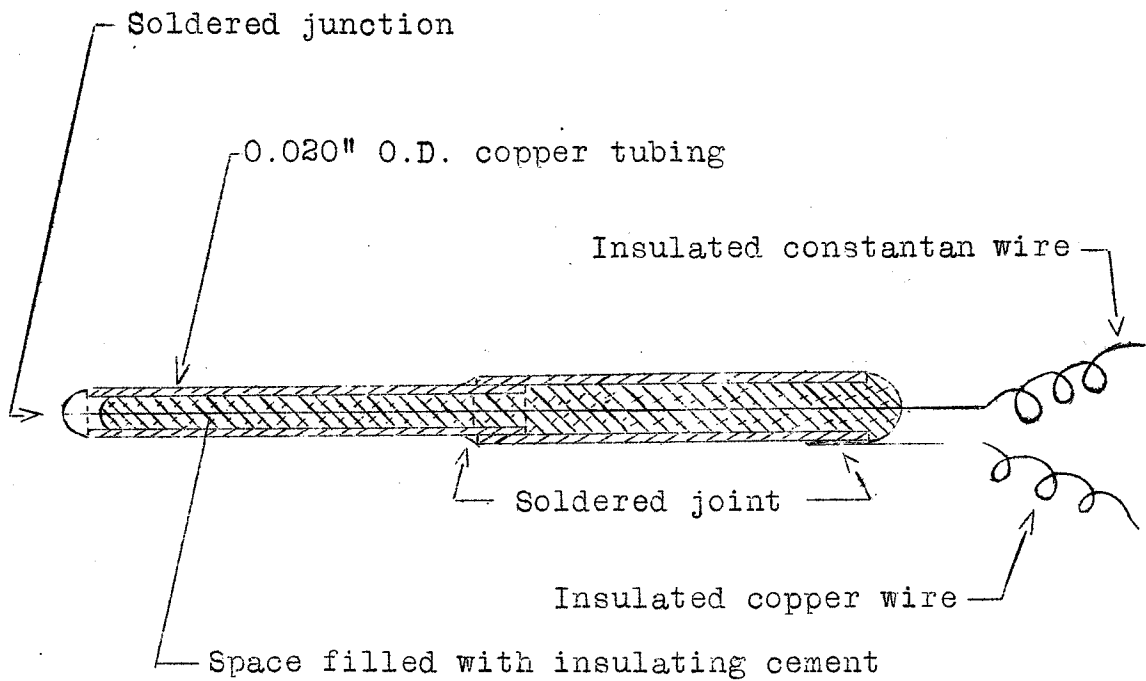


Figure 2.- Chordwise pressure distribution, $\alpha = 0^\circ$, $c_l = 0$, $R_c = 11 \times 10^6$ approximately.



Not to scale

Figure 3a.- Sketch of temperature mouse thermocouple tube.

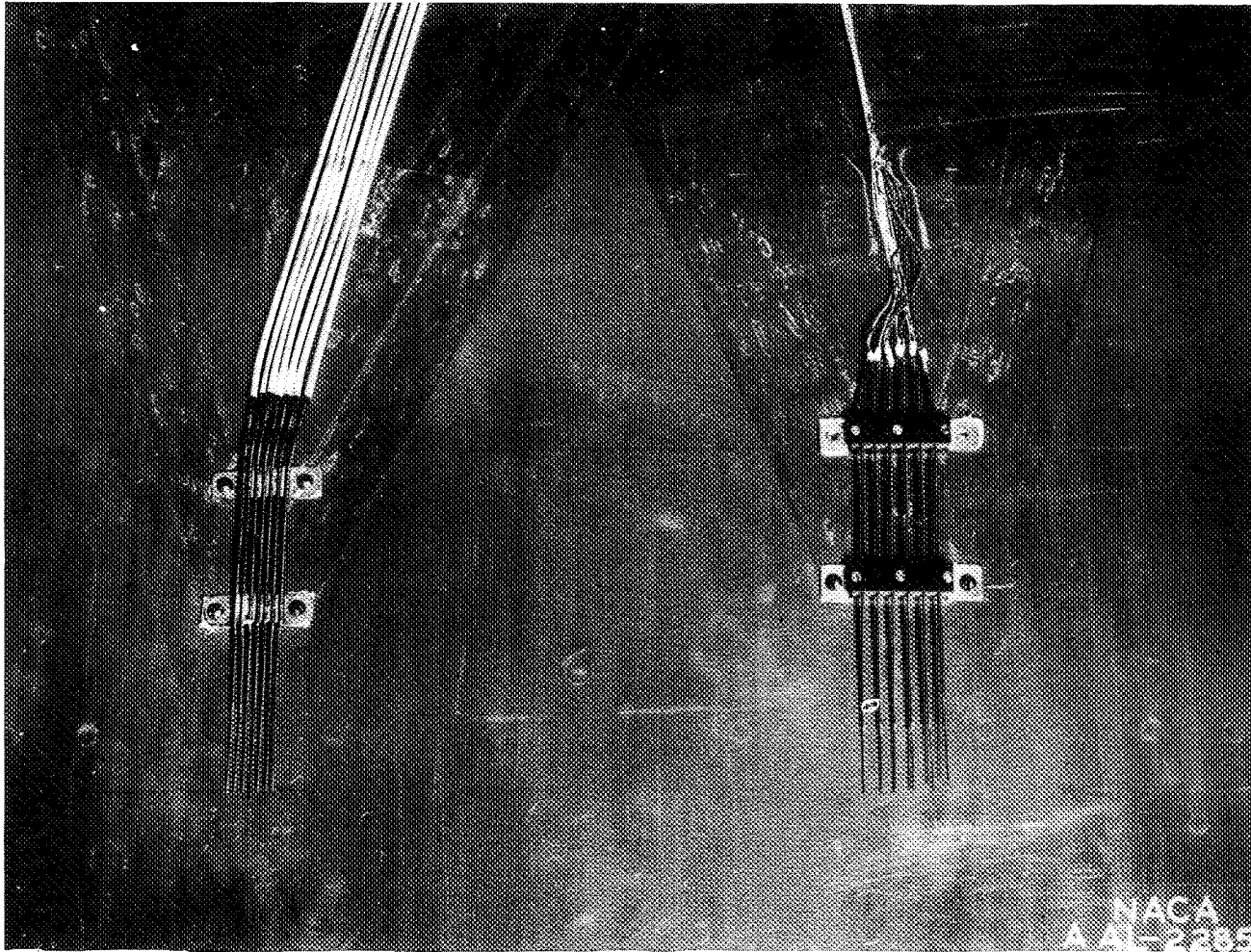


Figure 3b.- Detail view of temperature and velocity "mice".

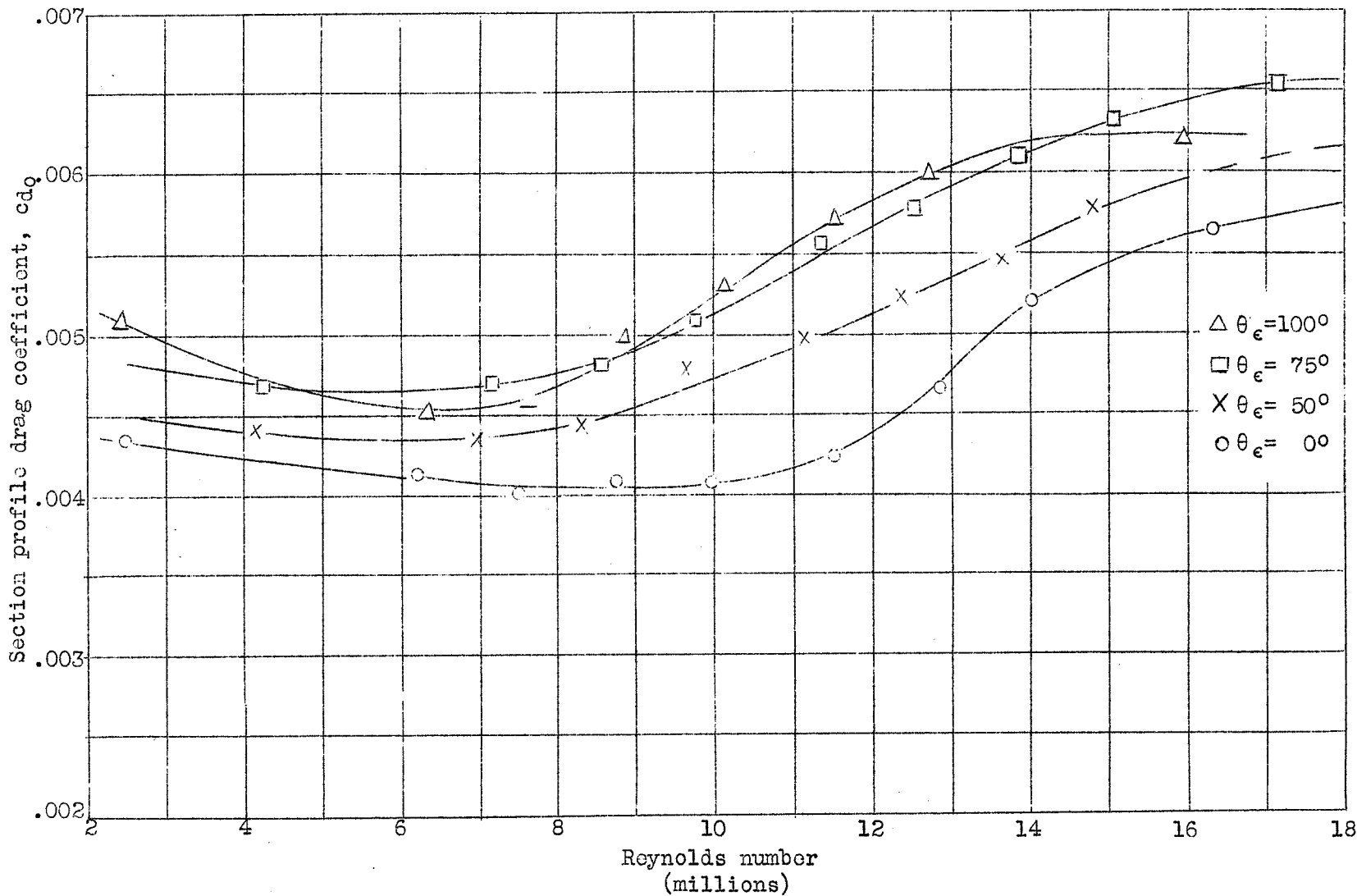


Figure 4.- Section drag coefficient variation with Reynolds number. Laminar run heated. $\alpha=0^\circ$.

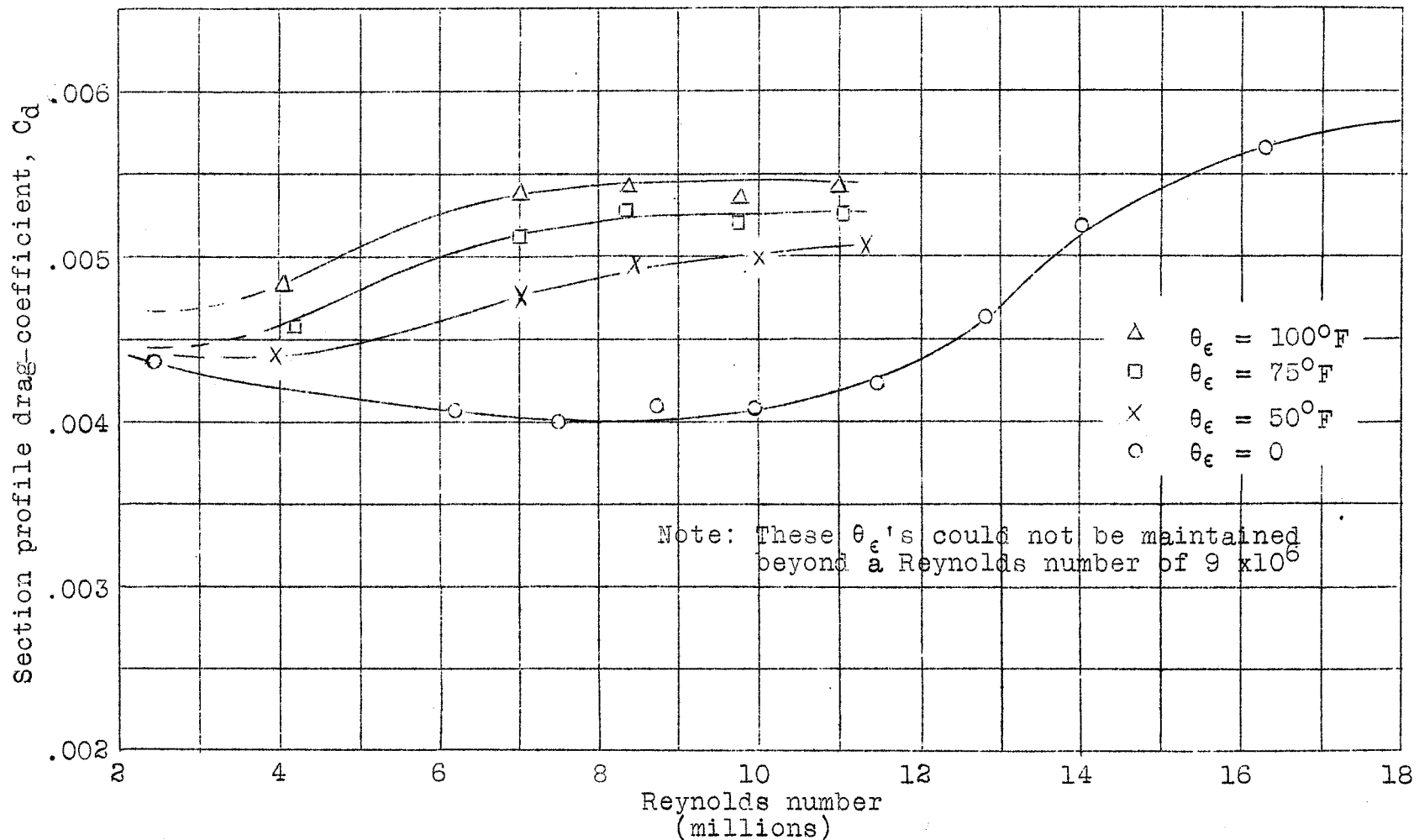


Figure 5.- Section profile drag-coefficient variation with Reynolds number for heat in section ahead of minimum pressure. $\alpha = 0^\circ$.

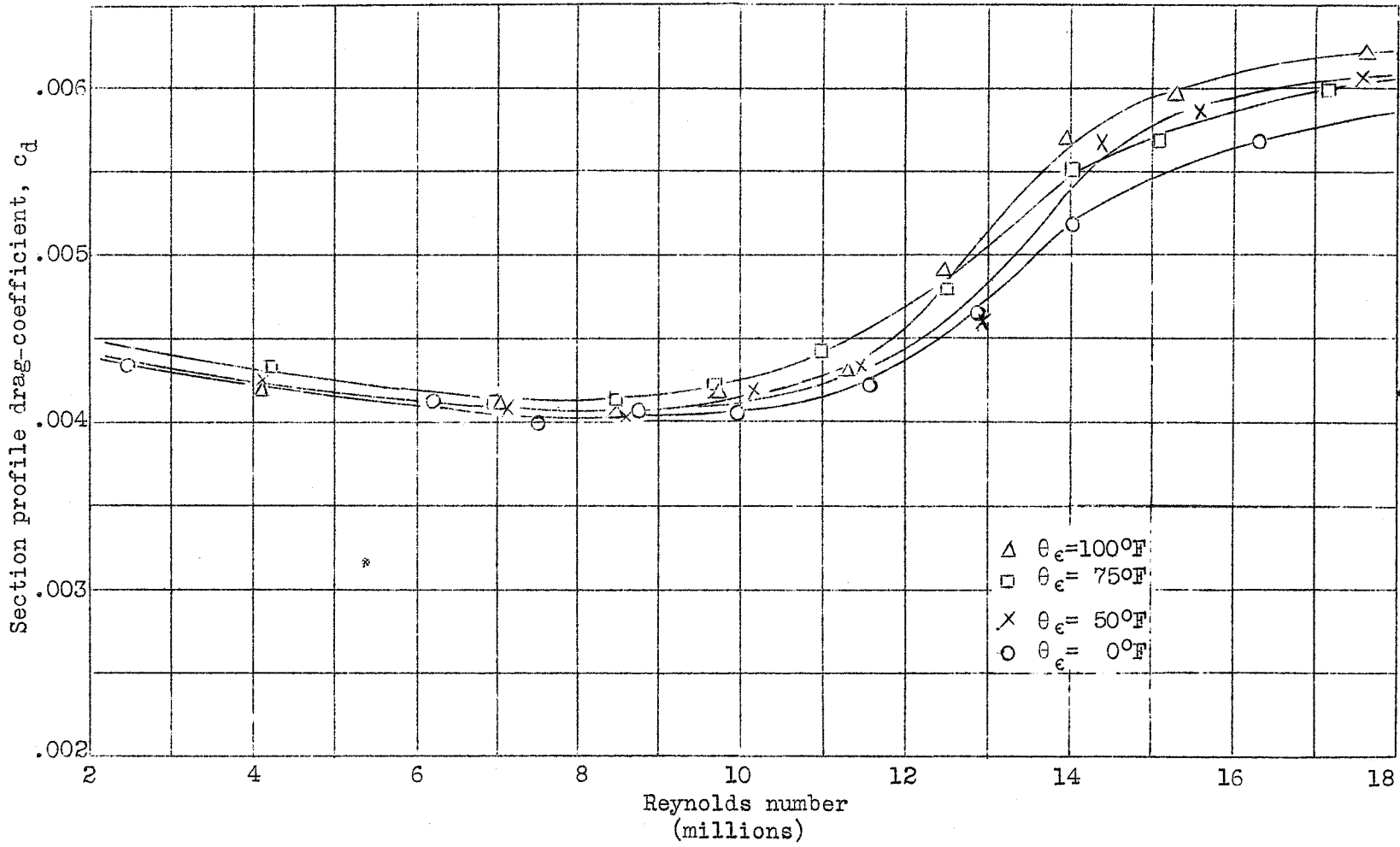


Figure 6.- Section drag-coefficient variation with Reynolds number. Nose section heated, $\alpha=0^\circ$.

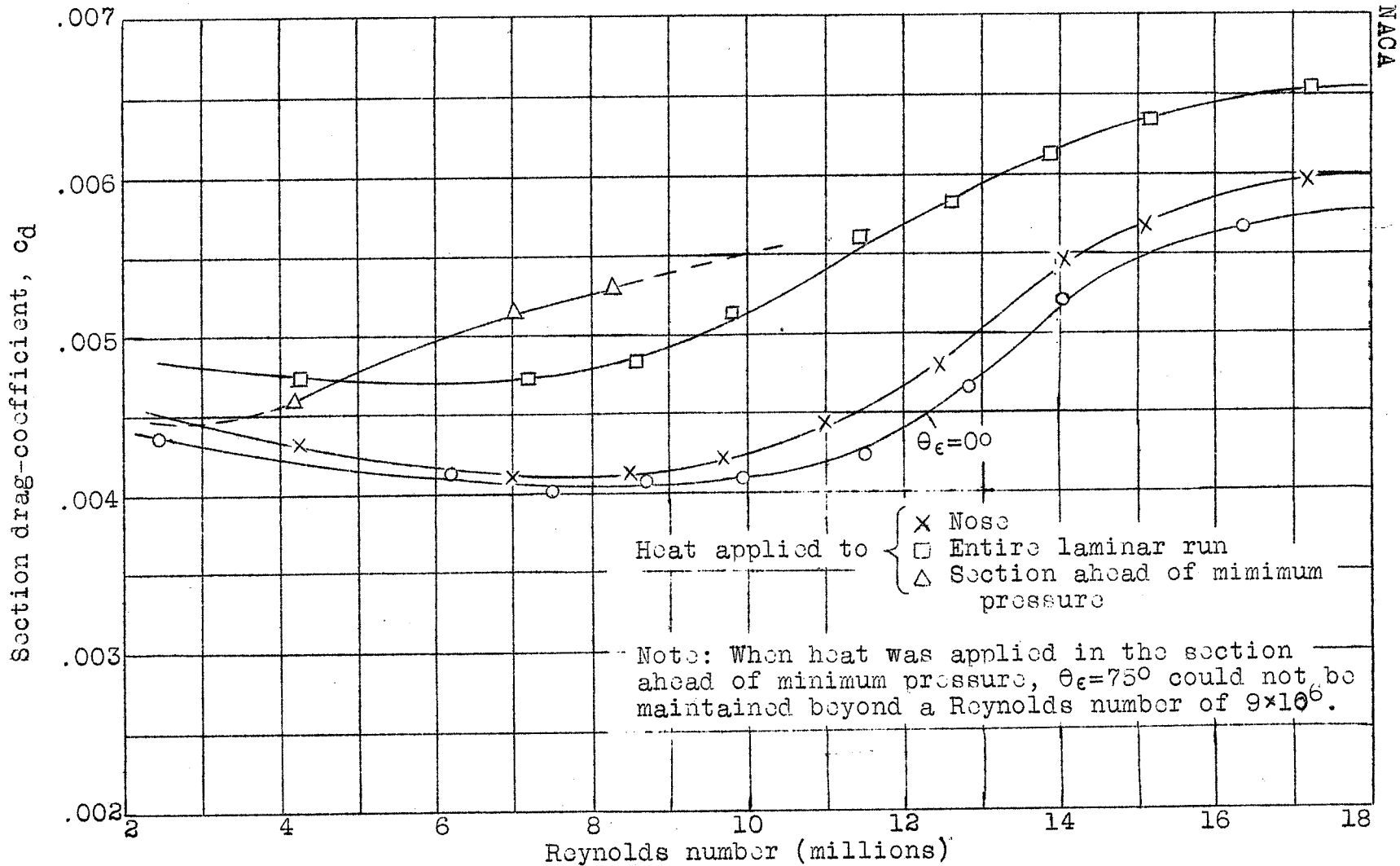


Figure 7.- Section profile drag-coefficient variation with Reynolds number for various portions of laminar run heated. $\theta_{\epsilon}=75^{\circ}$ F, $\alpha=0^{\circ}$, $c_l=0^{\circ}$.

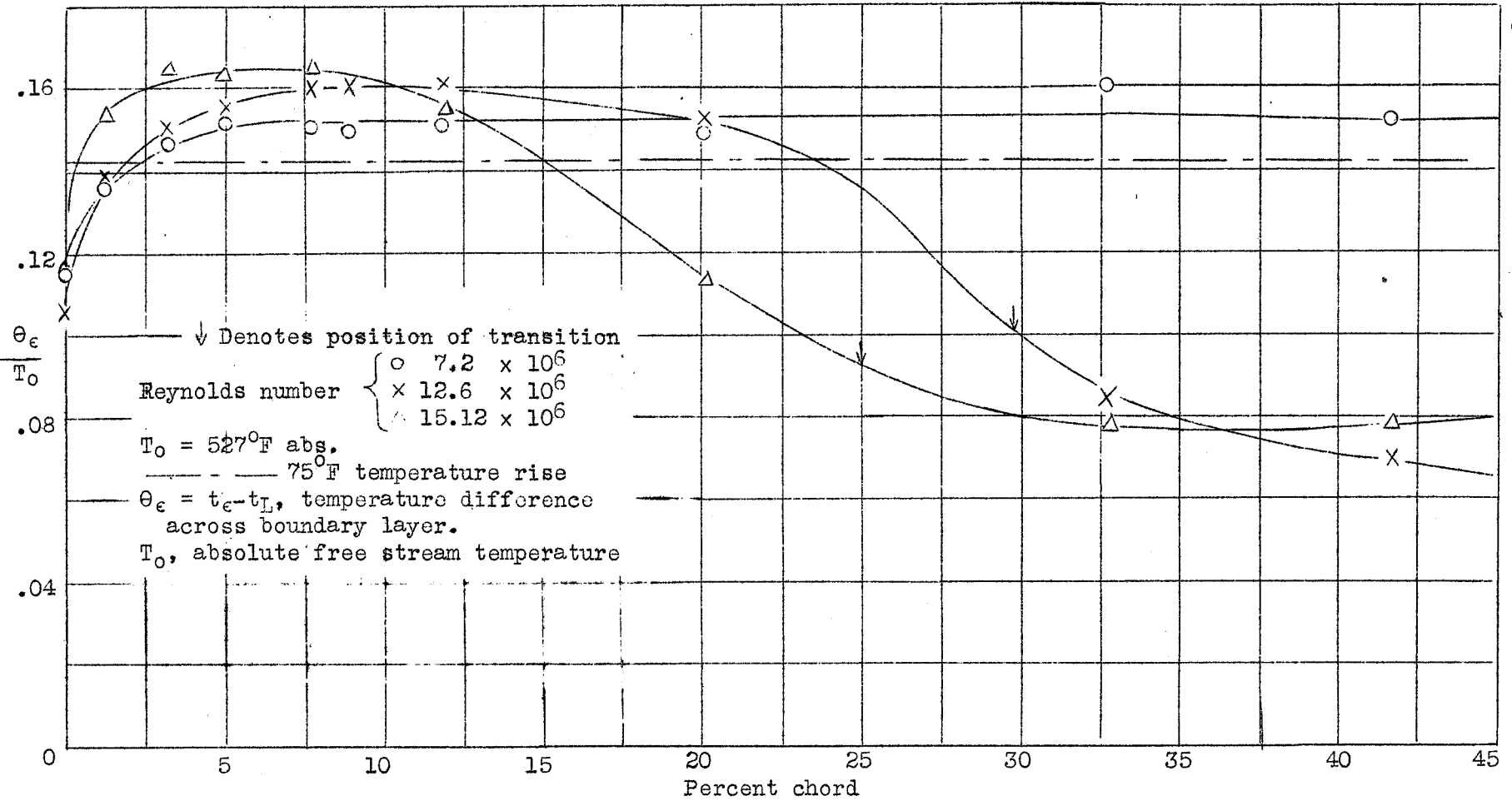


Figure 8.- Chordwise temperature distribution. Laminar run heated. $\theta_c = 75^\circ\text{F}$, $\alpha = 0^\circ$.

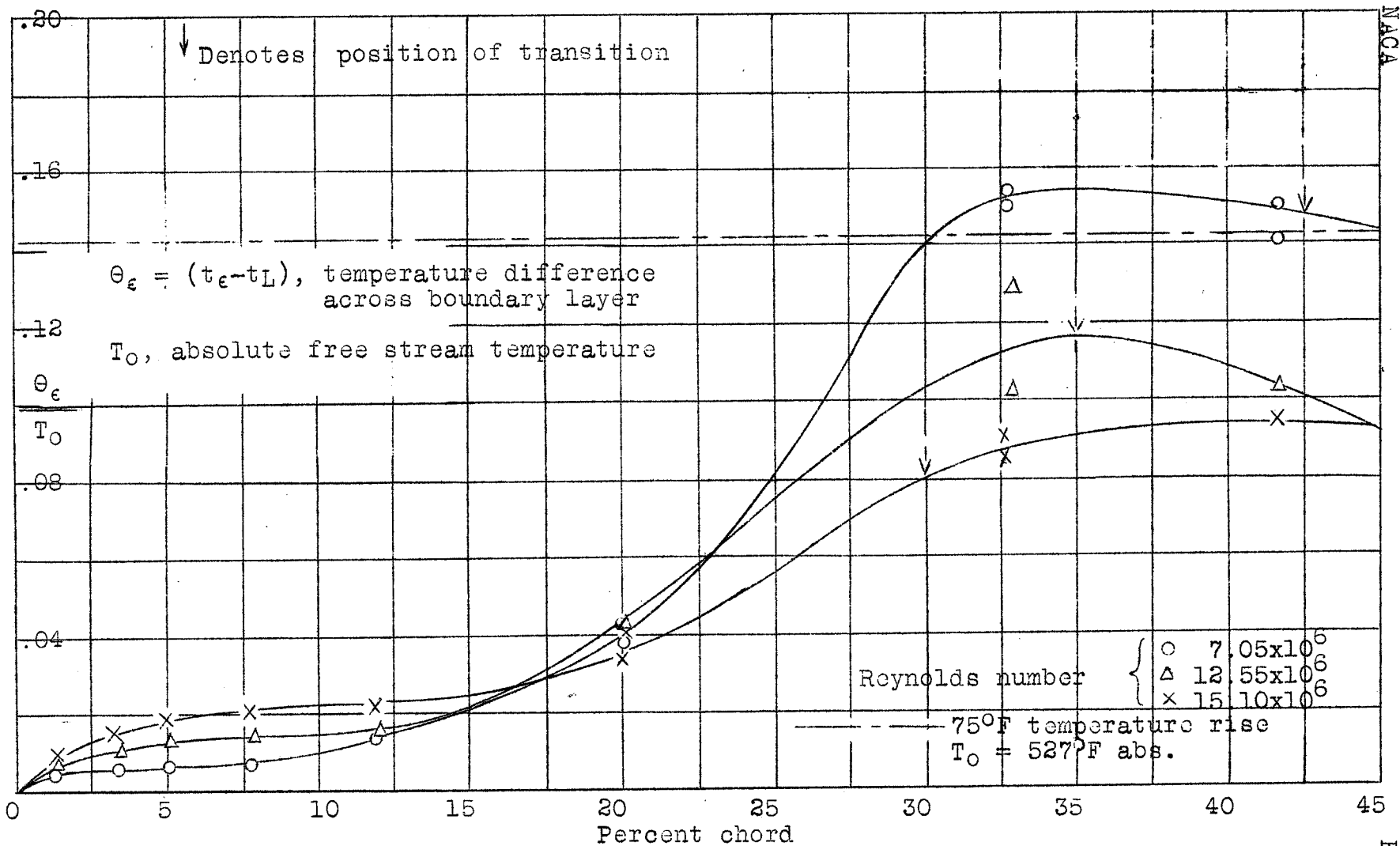


Figure 9.- Chordwise temperature distribution. Region just ahead of minimum pressure heated. $\theta_\epsilon = 75^\circ \text{F}$, $\alpha = 0^\circ$.

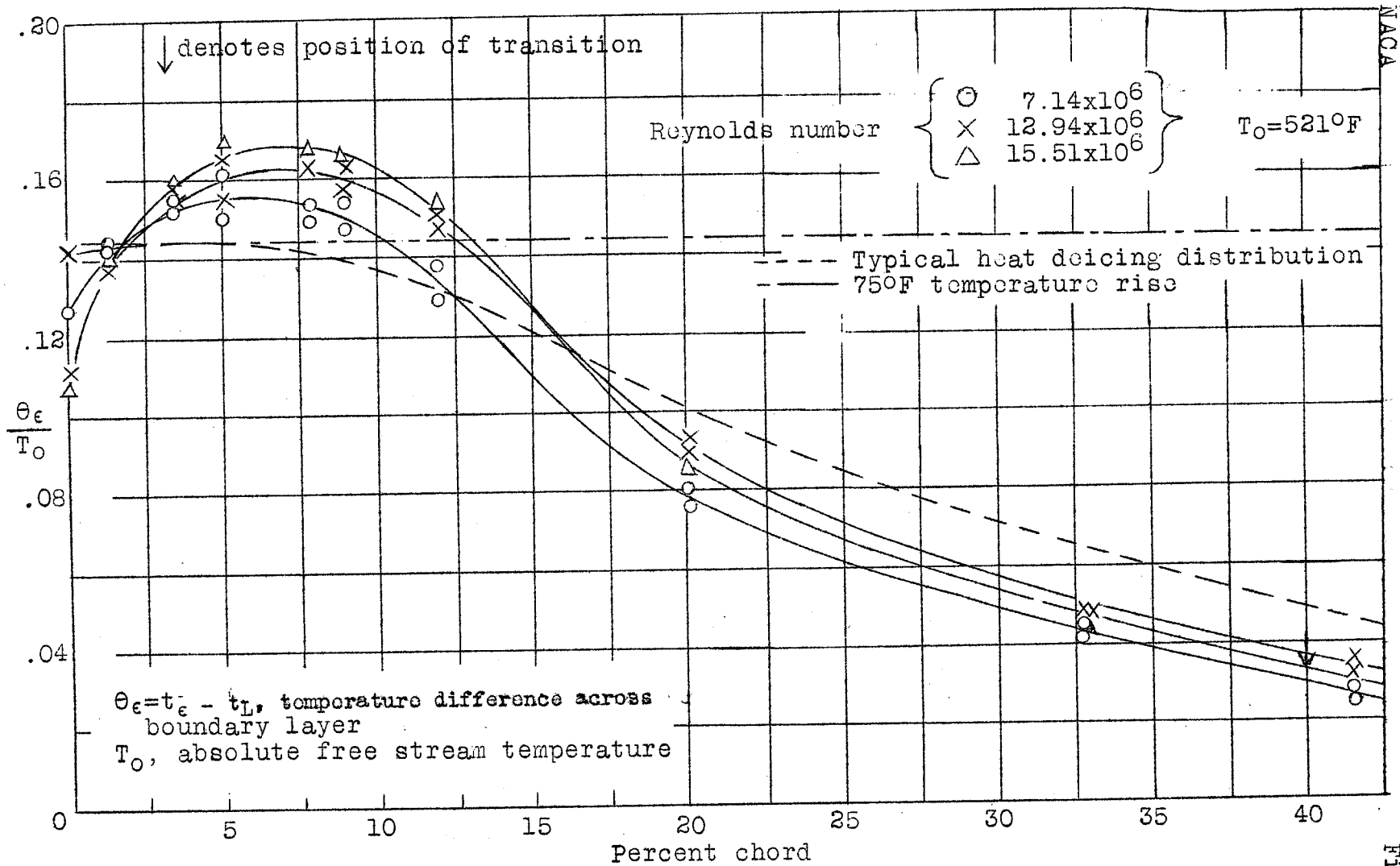


Figure 10.- Chordwise temperature distribution. Nose heated. $\theta_\epsilon = 75^\circ$, $\alpha = 0^\circ$

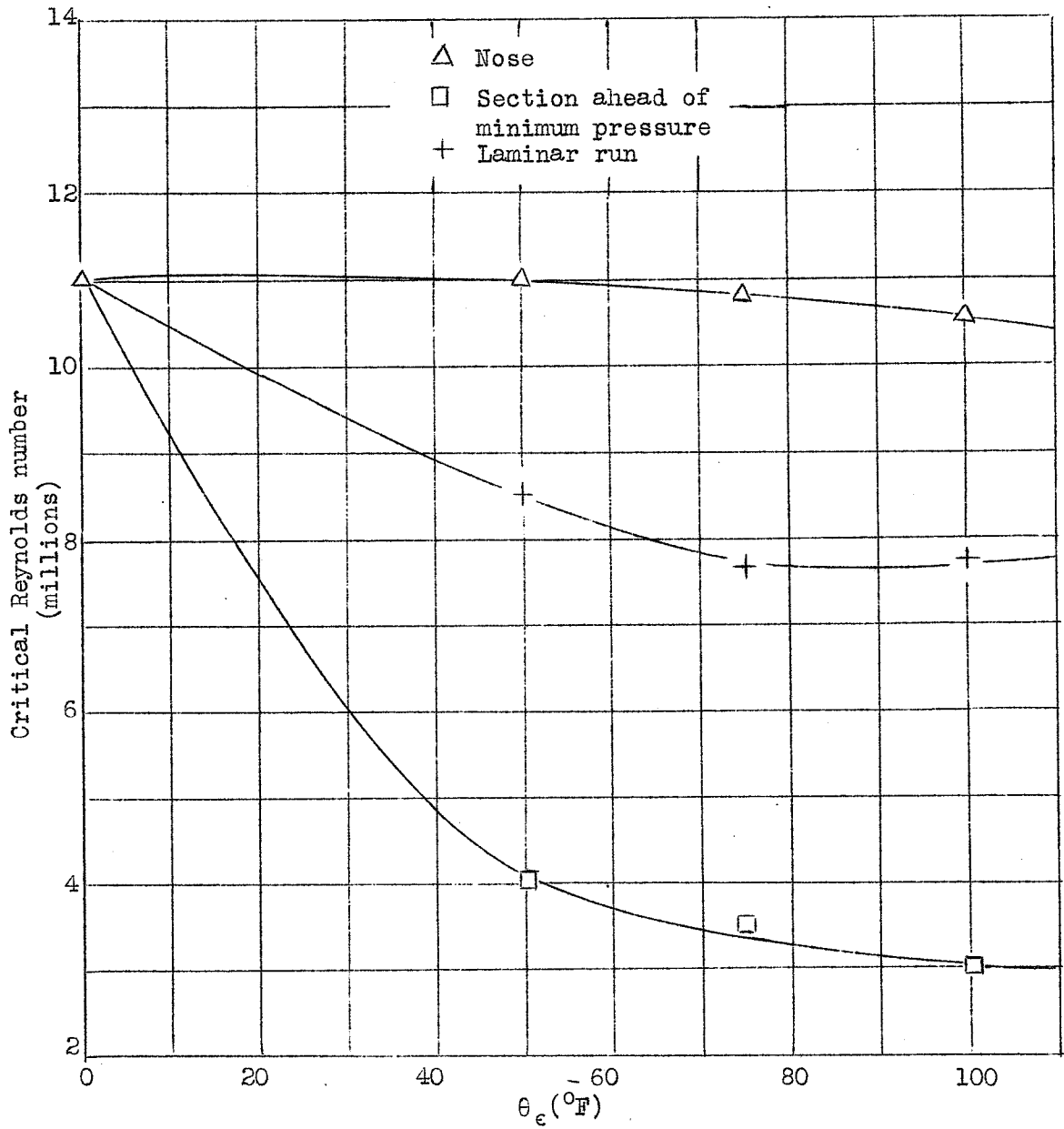


Figure 11.- Variation of critical Reynolds number with θ_c for various heat conditions.

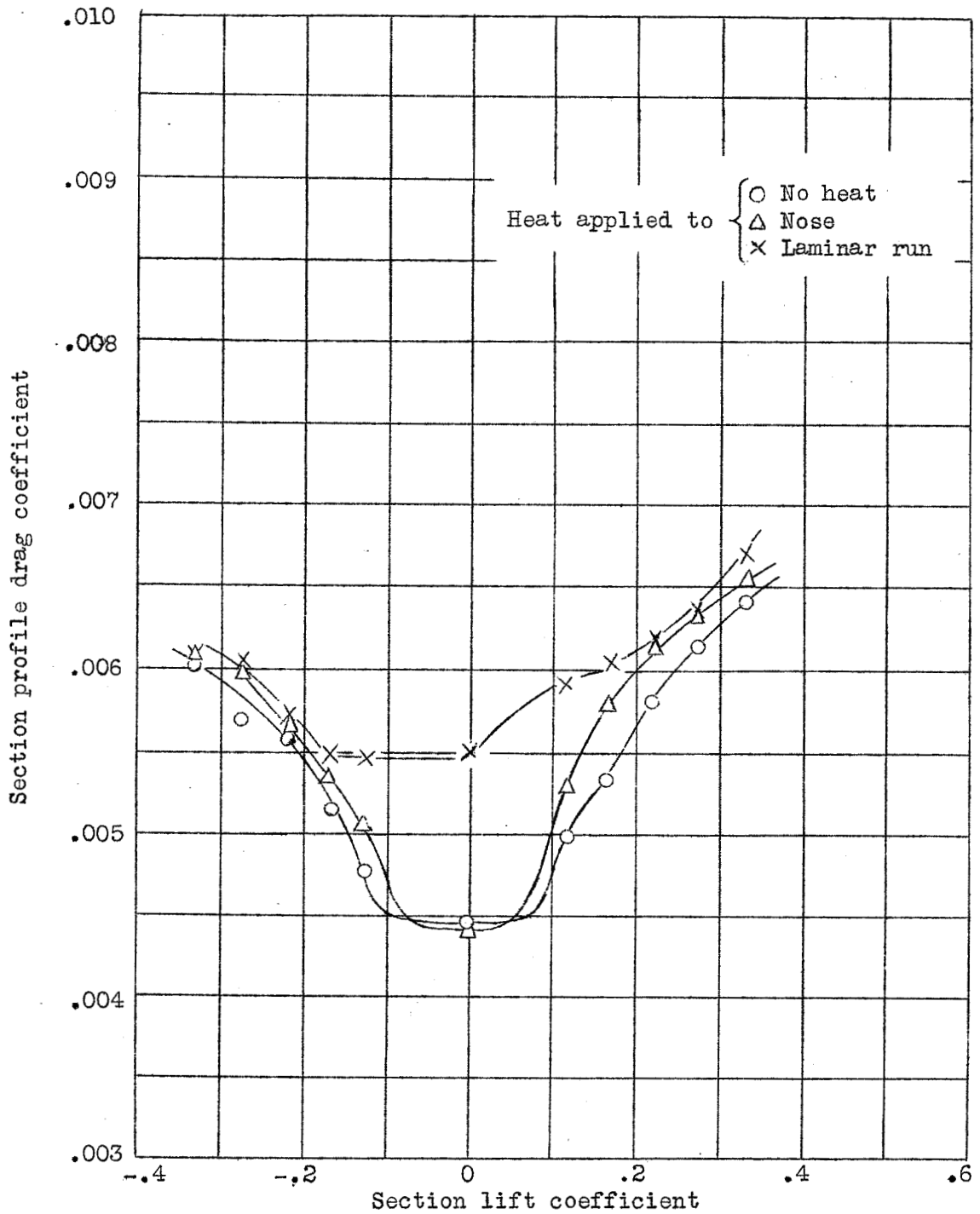


Figure 12.- Effect of heat on the range of lift coefficients over which low drag occurs. $\theta_c = 75^\circ\text{F}$, Reynolds number = 11.0×10^6 .

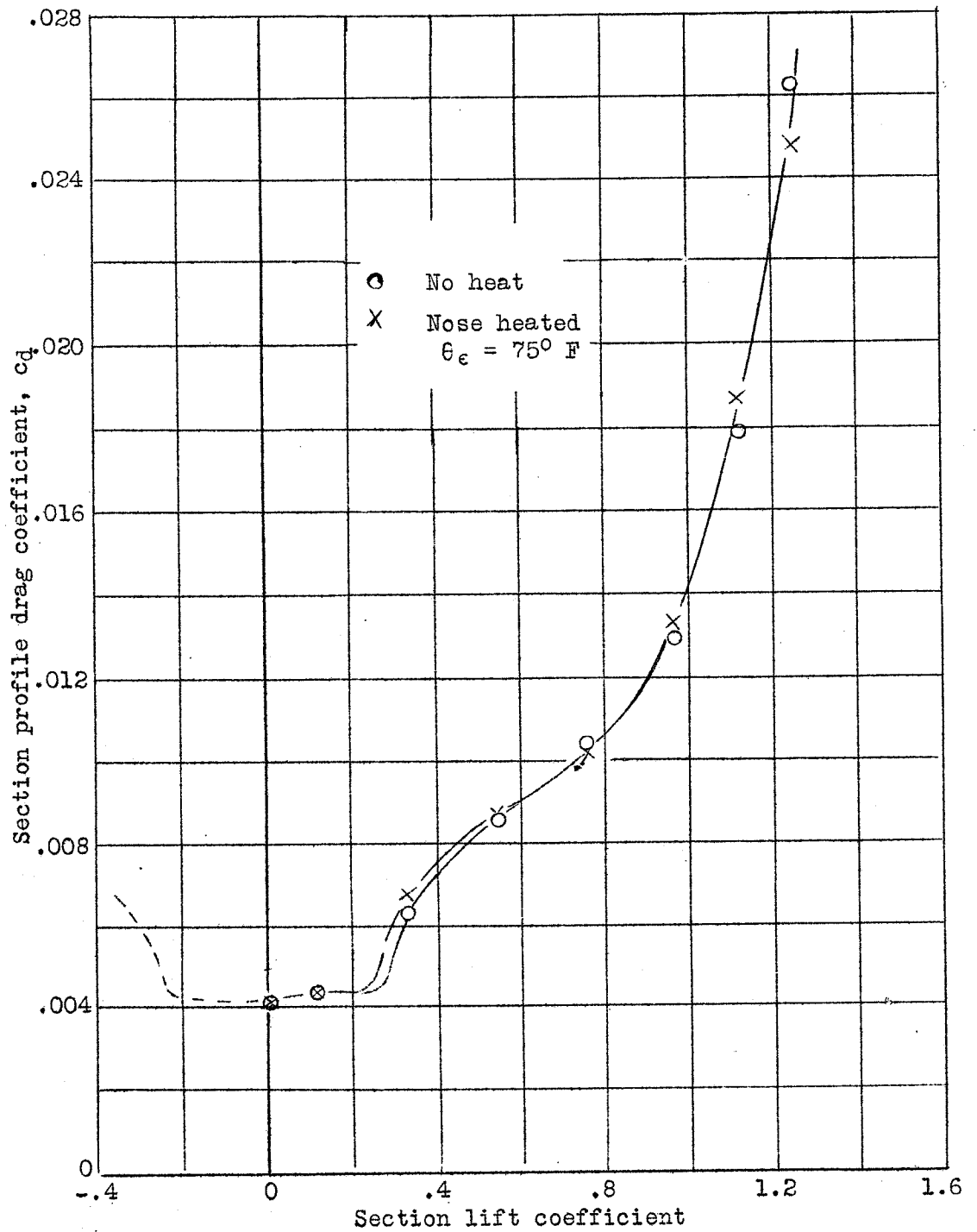


Figure 13.- Section drag-coefficient variation with section lift coefficient. Reynolds number 6.6×10^6 .

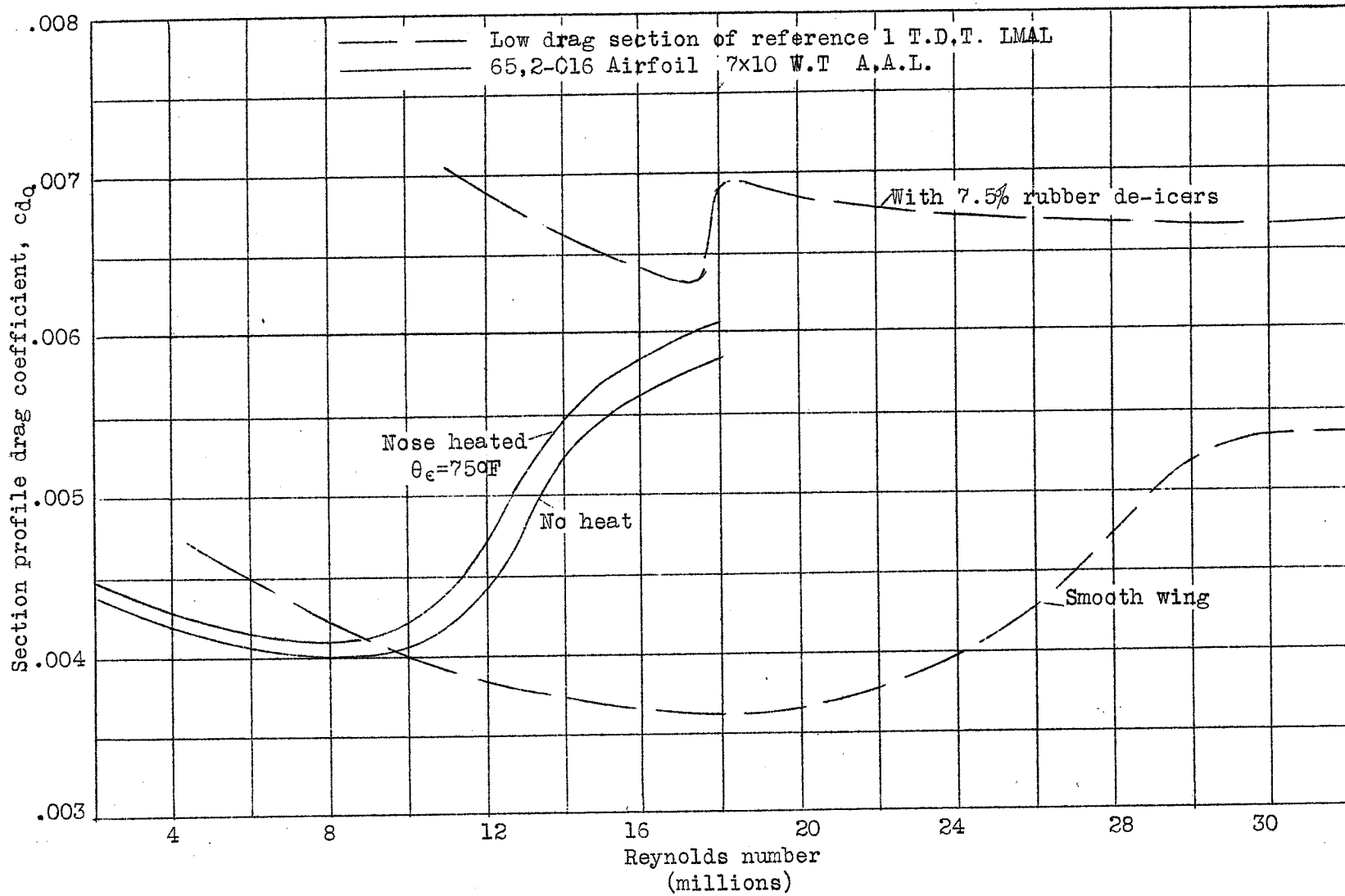


Figure 14.- Comparison of minimum drag variation with Reynolds number for rubber de-icers and heat de-icing.

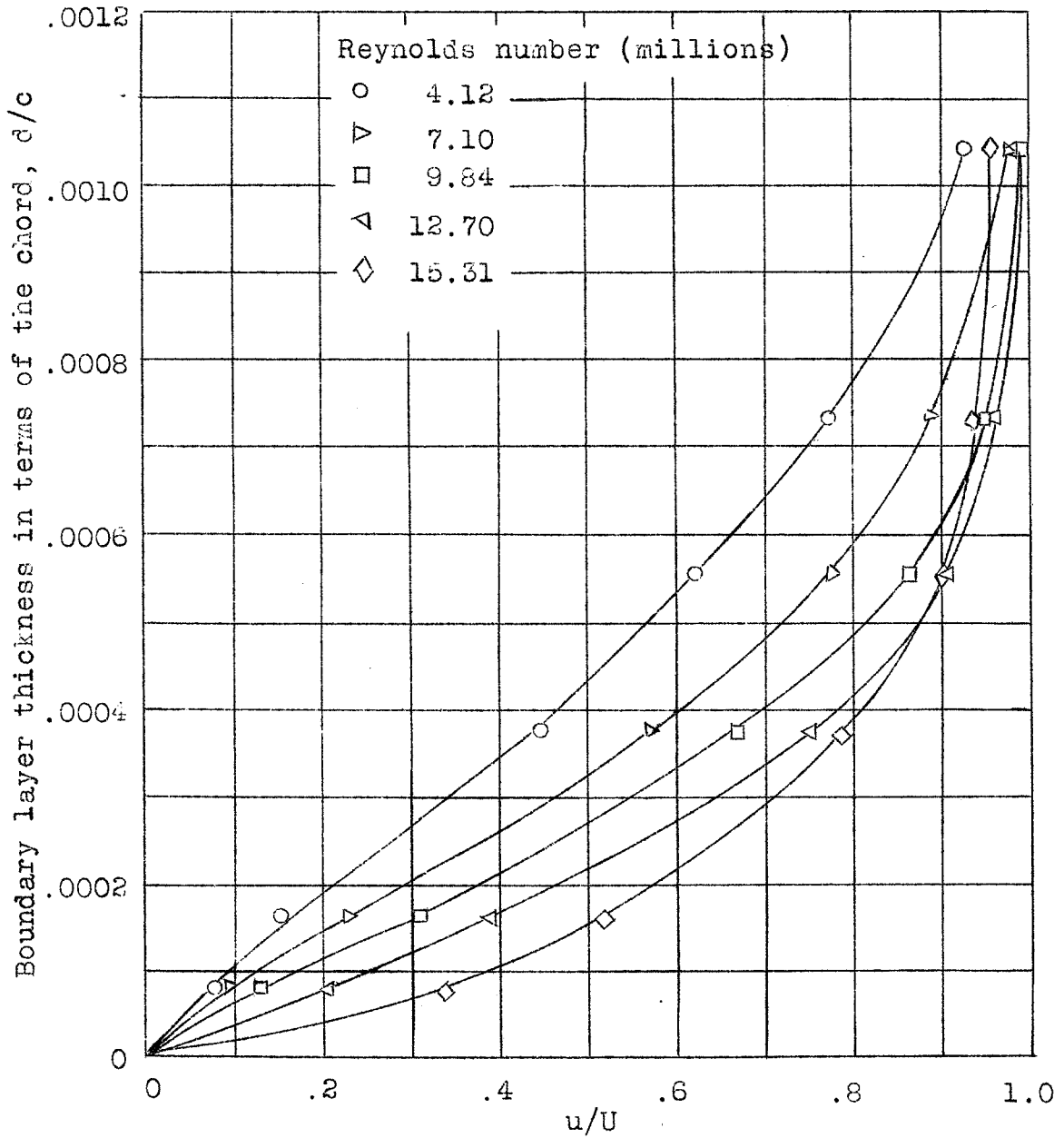


Figure 15.- Velocity boundary layers at 40-percent chord. No heat. $\alpha = 0^\circ$.

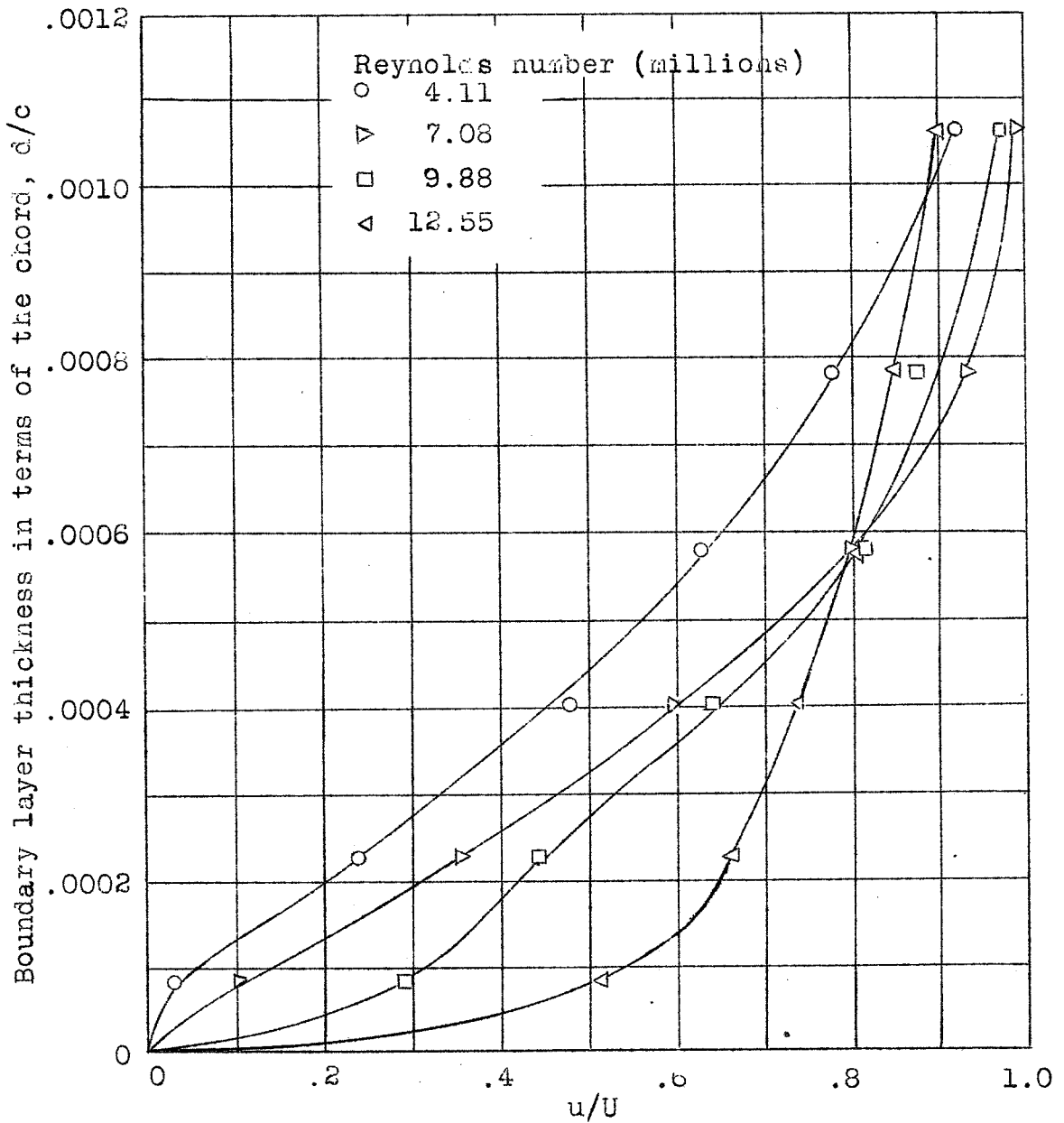


Figure 16.- Velocity boundary layers at 40-percent chord. Laminar run heated. $\theta_\epsilon = 75^\circ\text{F}$, $\alpha = 0^\circ$.

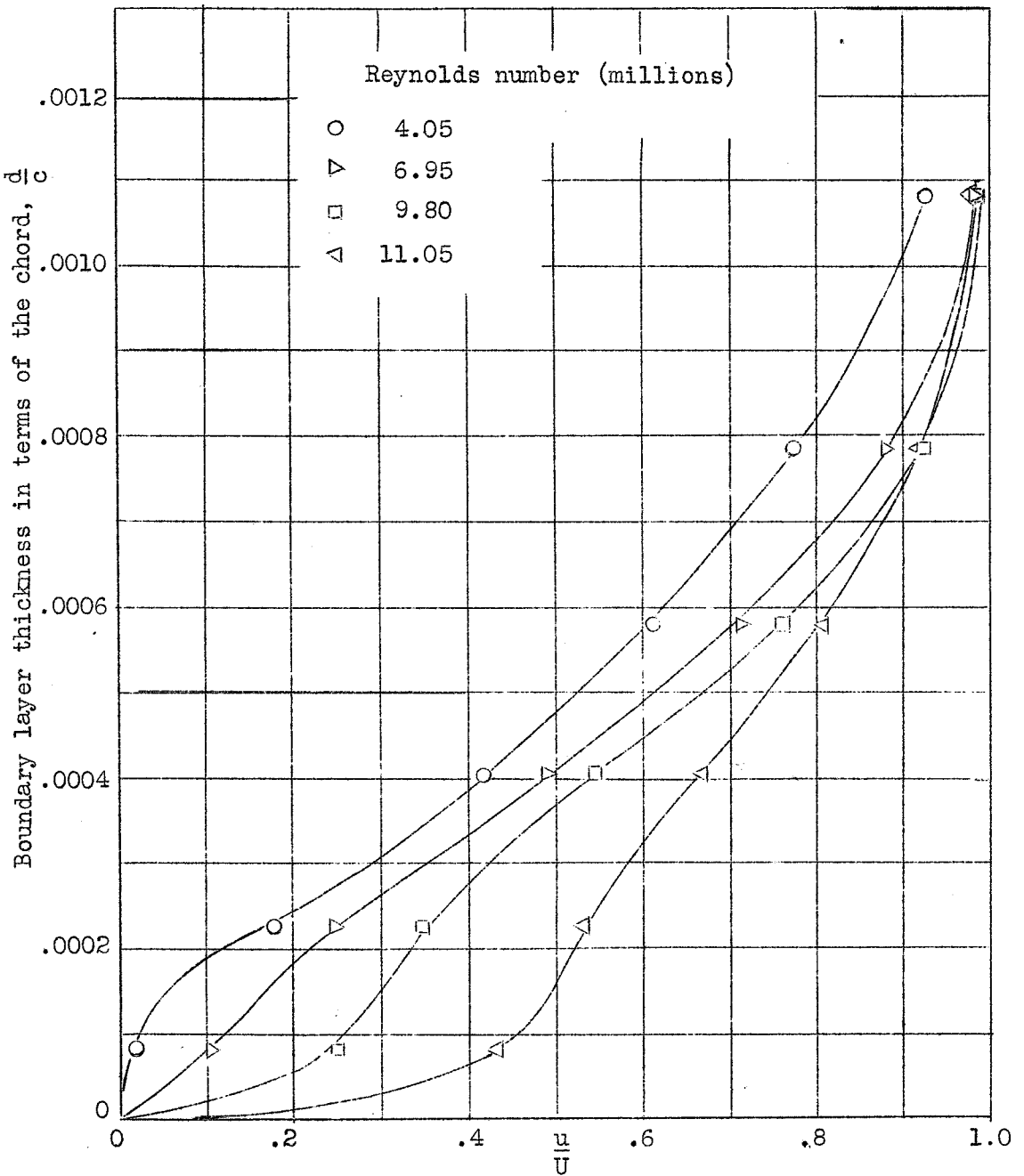


Figure 17.- Velocity boundary layers at 40-percent chord. Heat at minimum pressure. $\theta_c = 75^\circ \text{ F}$, $\alpha = 0^\circ$.

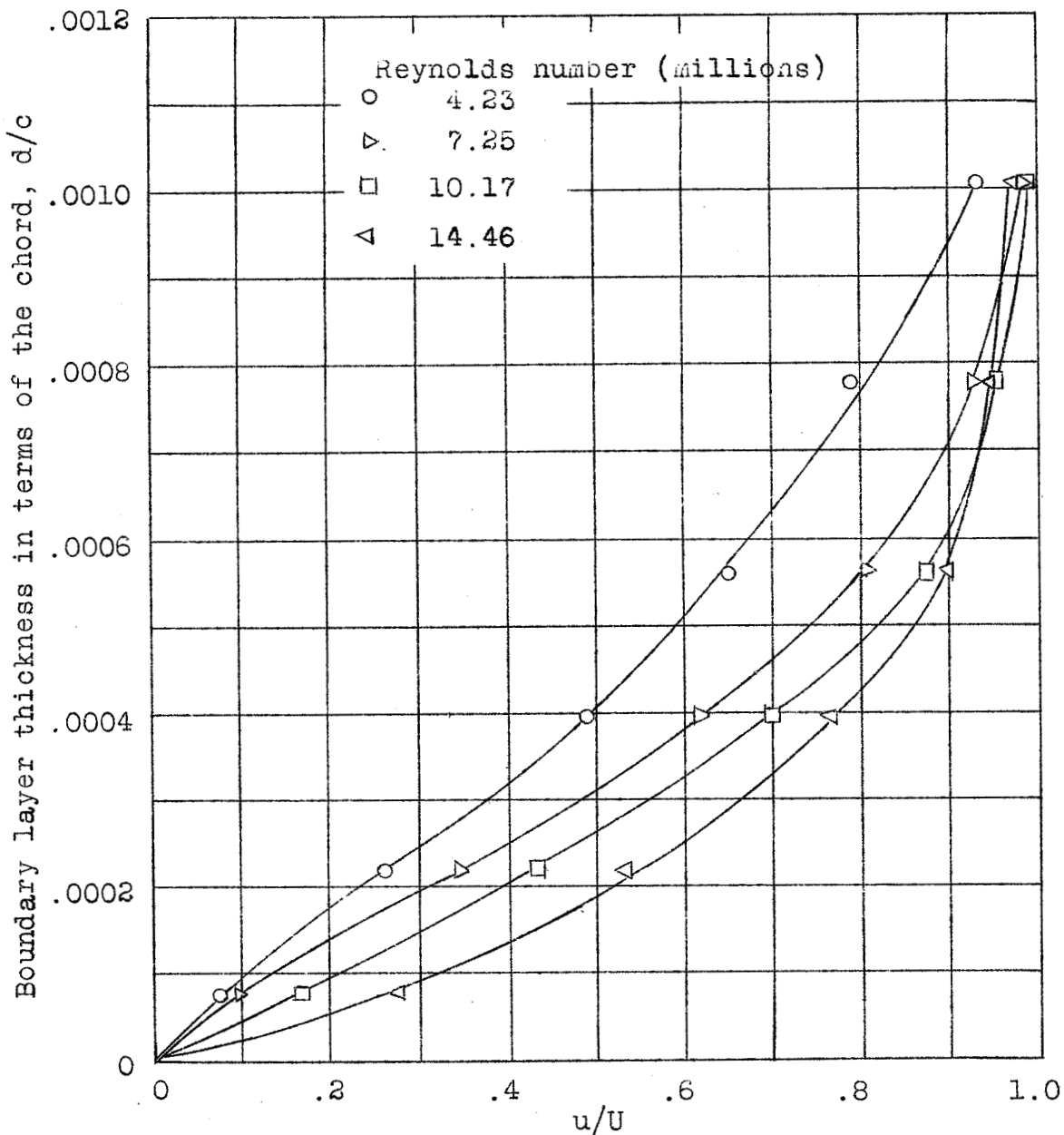


Figure 18.- Velocity boundary layers at 40-percent chord. Nose only heated. $\theta_c = 75^\circ\text{F}$, $\alpha = 0^\circ$.

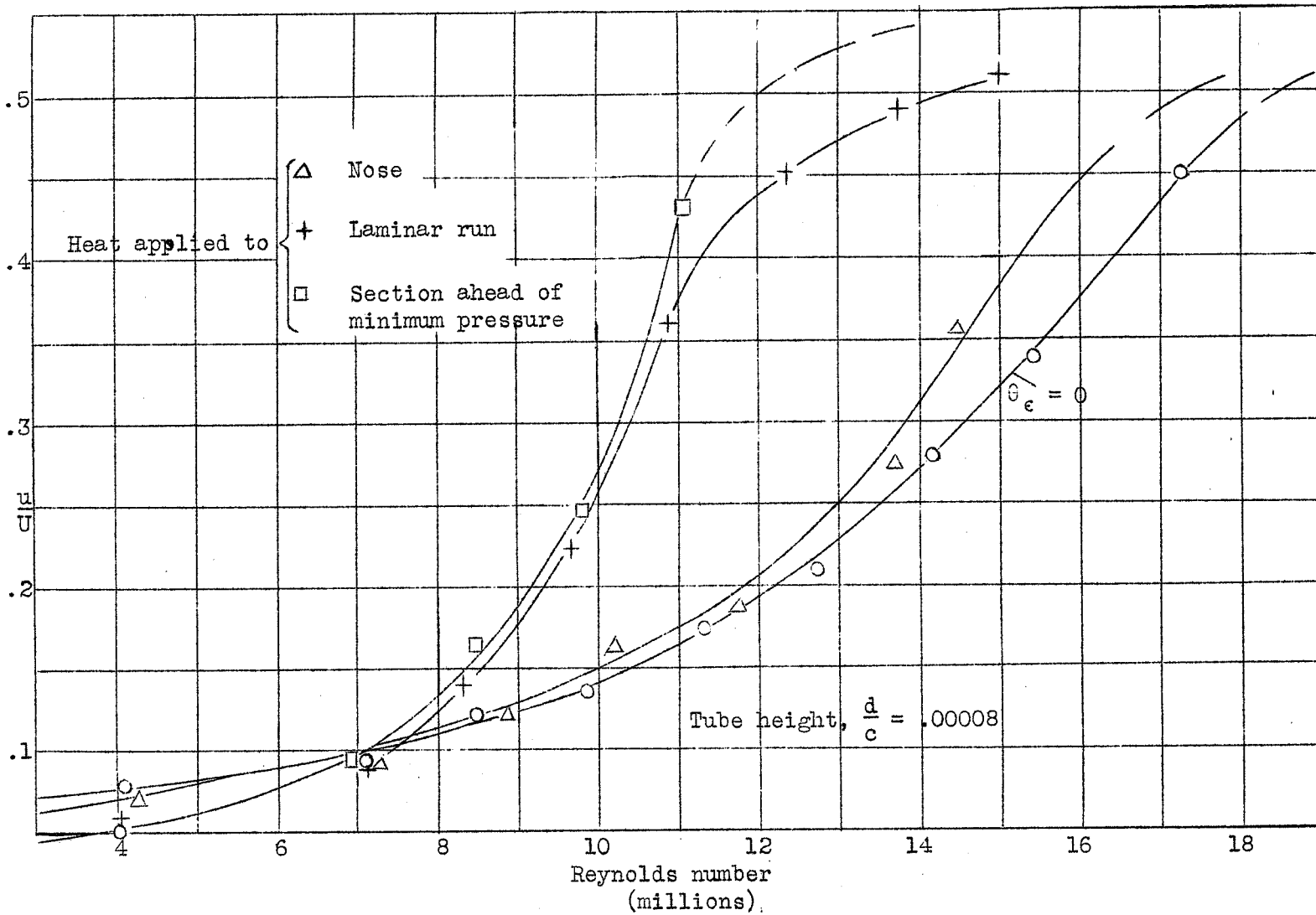


Figure 19.- Mouse surface-tube reading against Reynolds number. Mouse at 40-percent chord. $\alpha = 0^\circ$, $\theta_{\epsilon} = 75^\circ \text{ F.}$

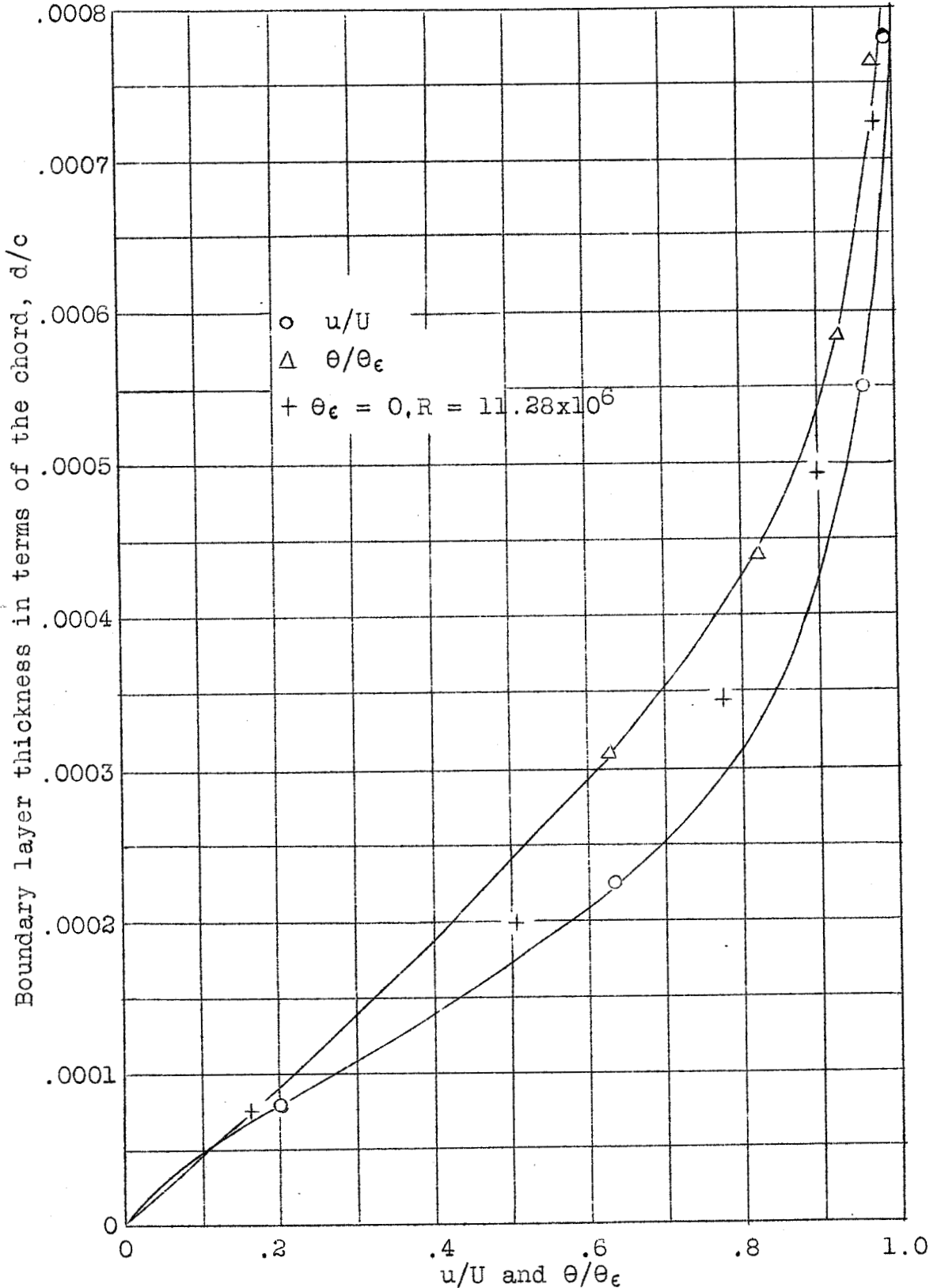


Figure 20.- Velocity and temperature boundary layers at 29-percent chord for the laminar run heated. $\alpha = 0^\circ$, Reynolds number = 11.01×10^6 , $\theta_\epsilon = 75^\circ\text{F}$.

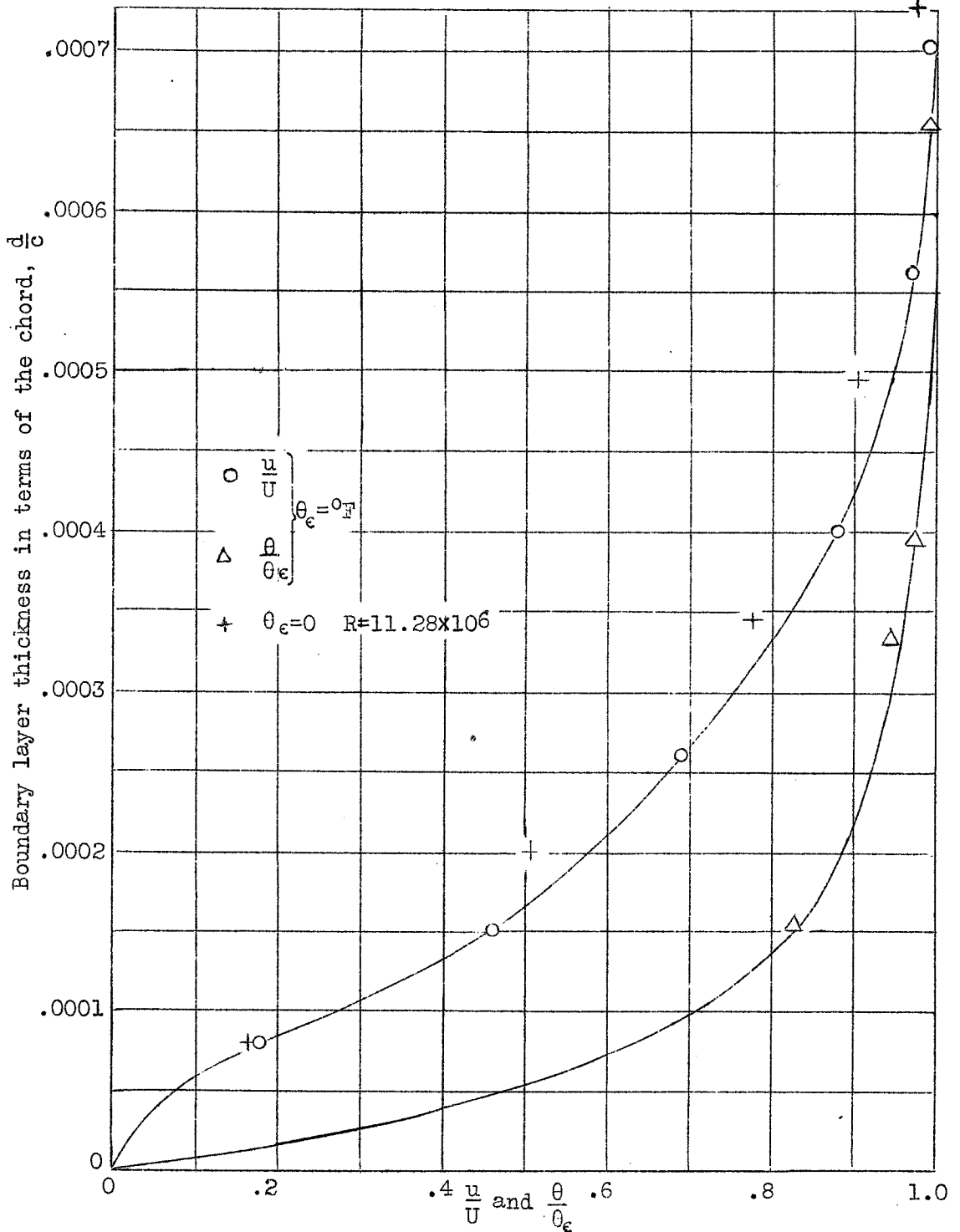


Figure 21.- Velocity and temperature boundary layers at 29-percent chord for heat applied to section ahead of minimum pressure position. $\alpha = 0^\circ$, Reynolds number = 10.89×10^6 , $\theta_e = 75^\circ F$.

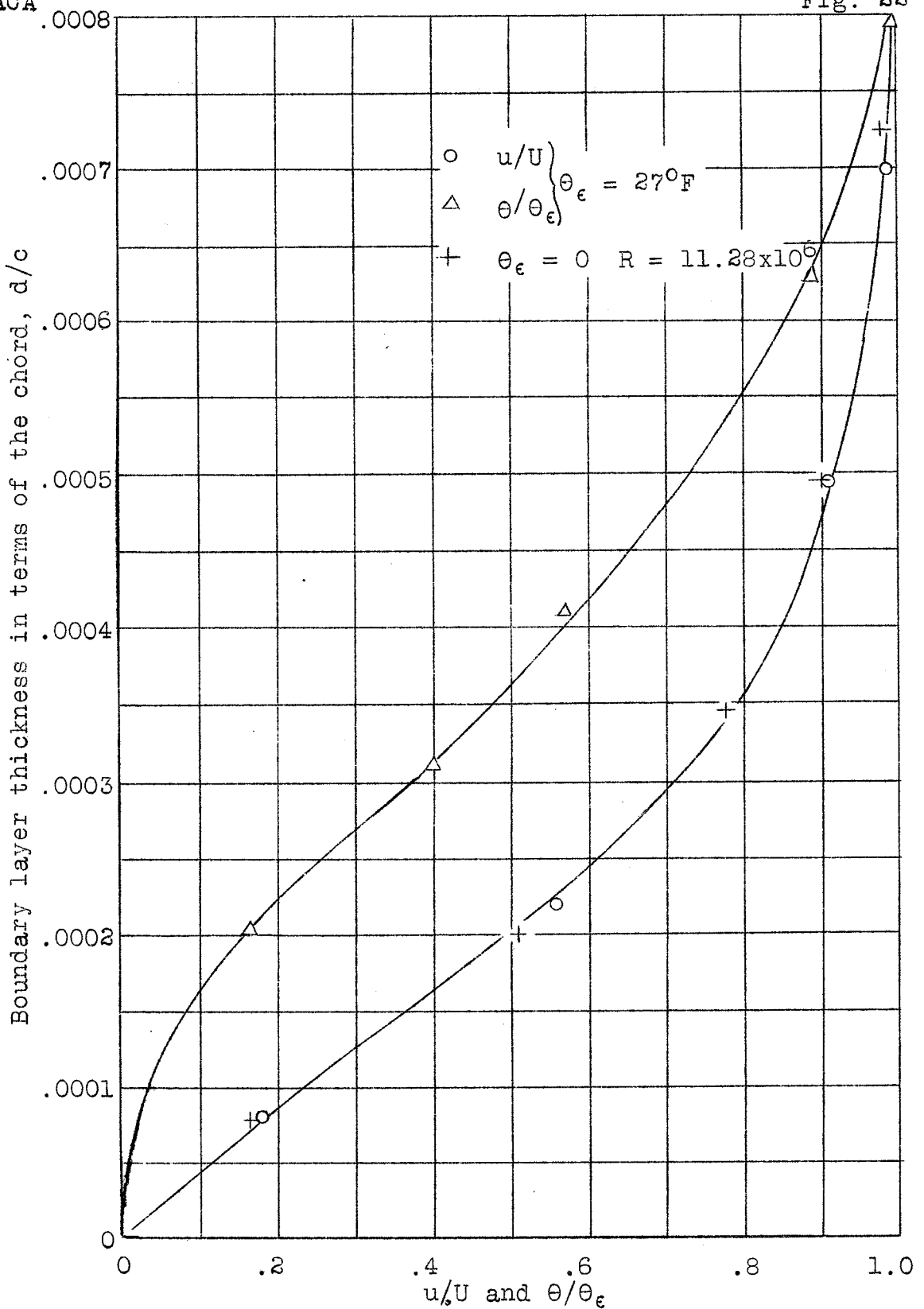


Figure 22.- Velocity and temperature boundary layers at 29-percent chord. Nose heated. $\alpha = 0^\circ$. Reynolds number = 11.45×10^6 , $\theta_\epsilon = 75^\circ$.

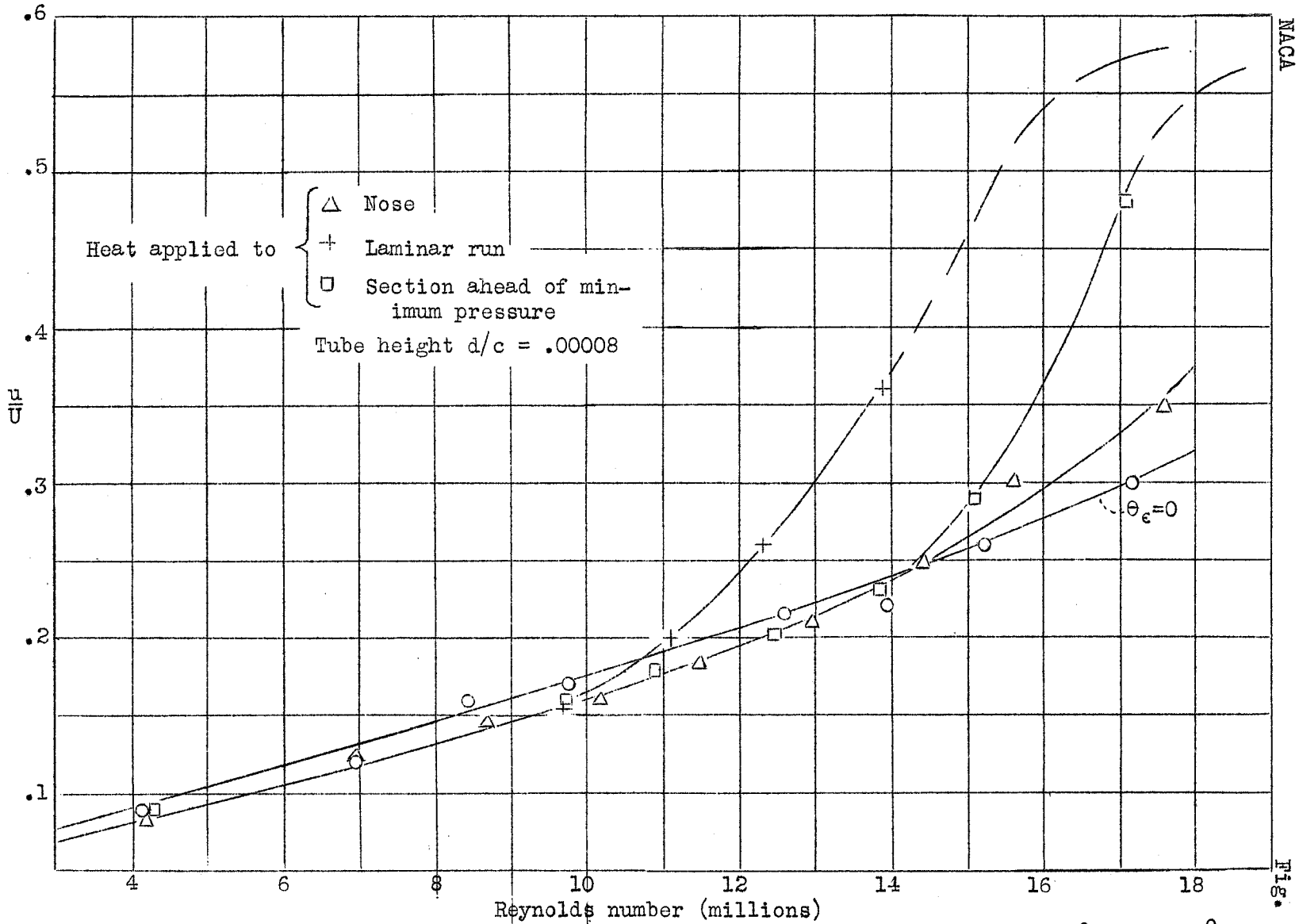


Figure 23.- Mouse surface-tube reading vs Reynolds number. Mouse at 29-percent chord. $\alpha = 0^{\circ}$, $\theta_{\epsilon} = 75^{\circ}\text{F}$.

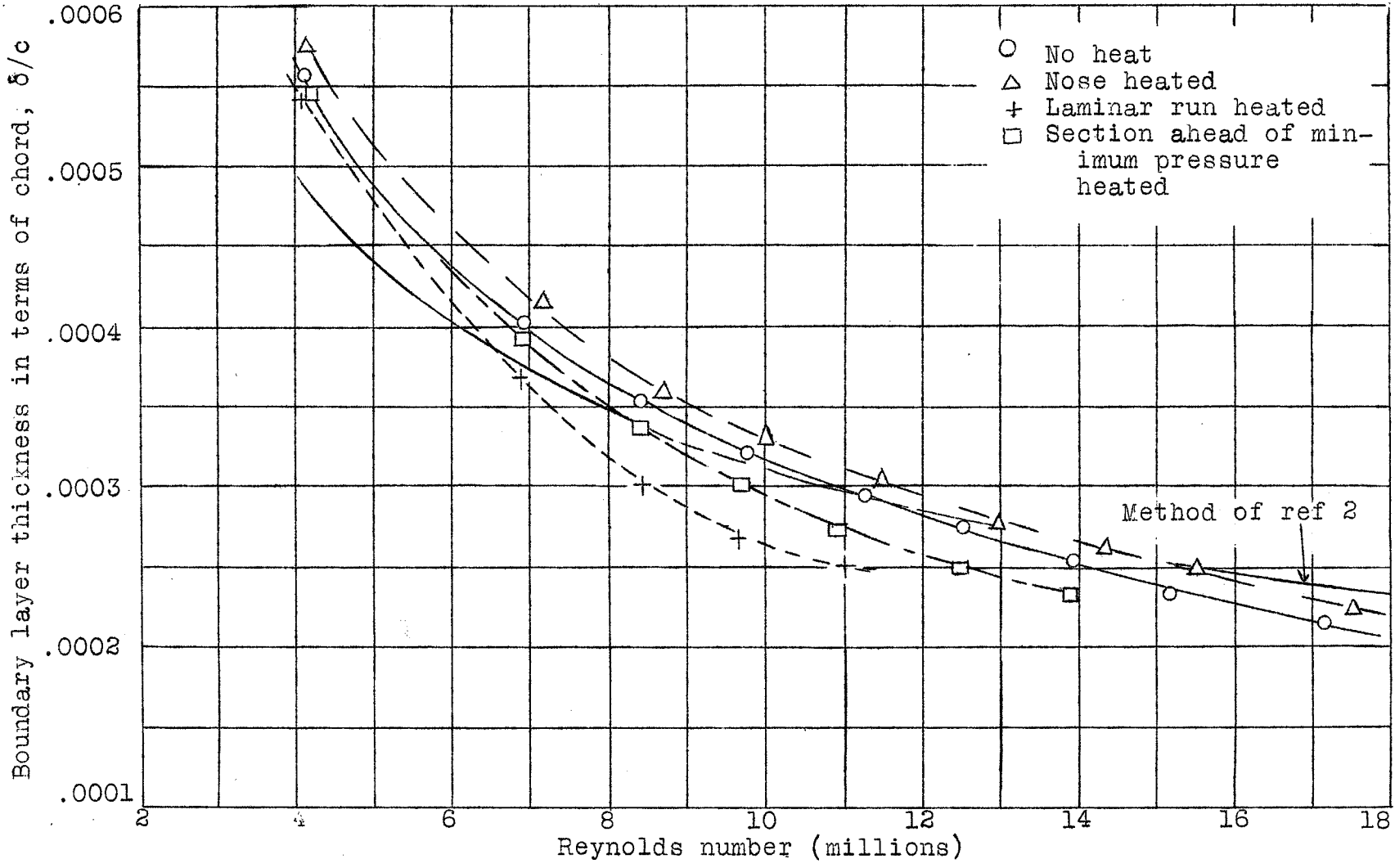


Figure 24.- Boundary-layer thickness variation with Reynolds number, 29-percent chord.
 $\alpha = 0^\circ$, $\theta_c = 75^\circ\text{F}$.

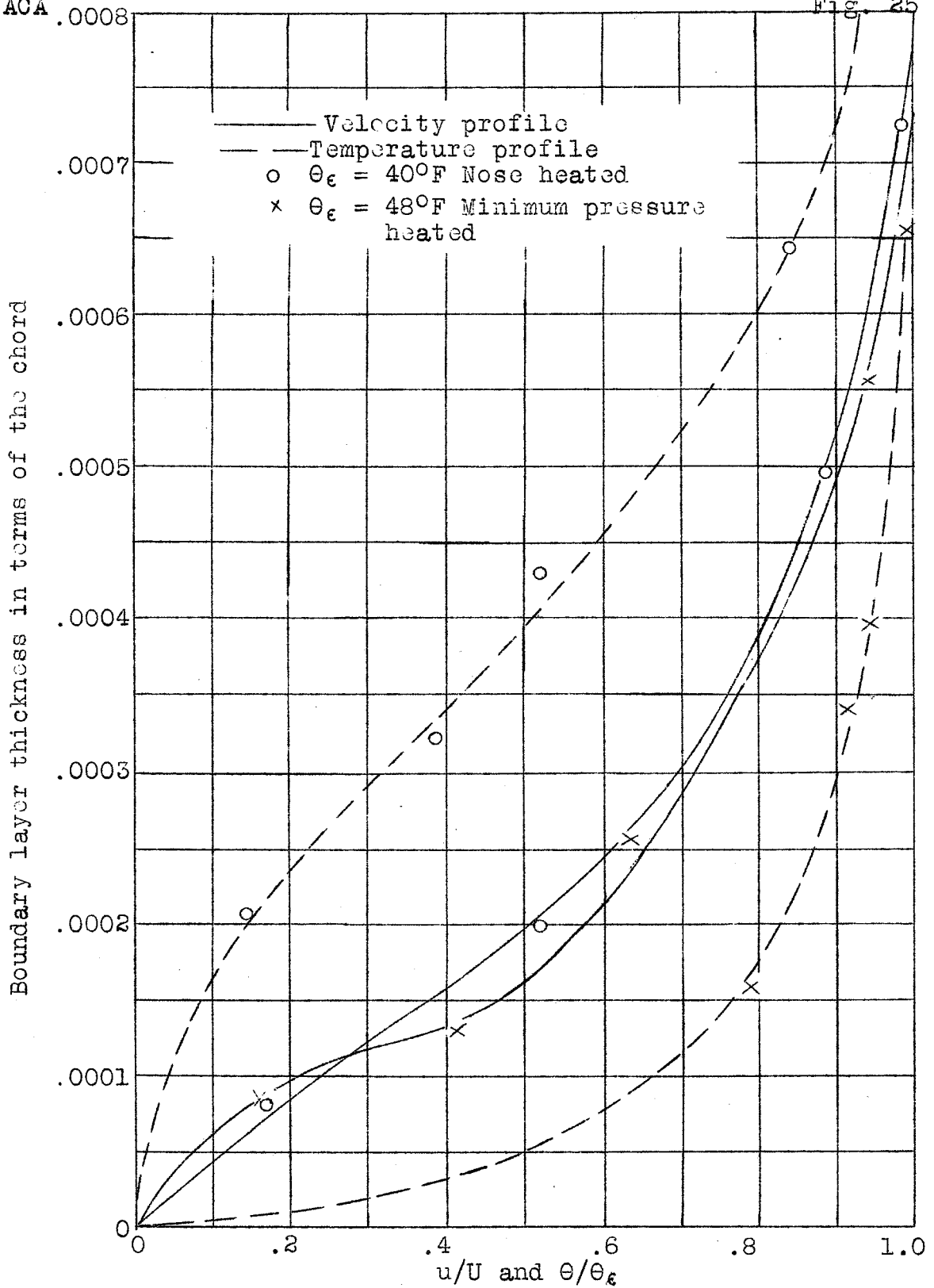


Figure 25.- Variation of velocity profile with type of temperature distribution for same θ_ϵ .

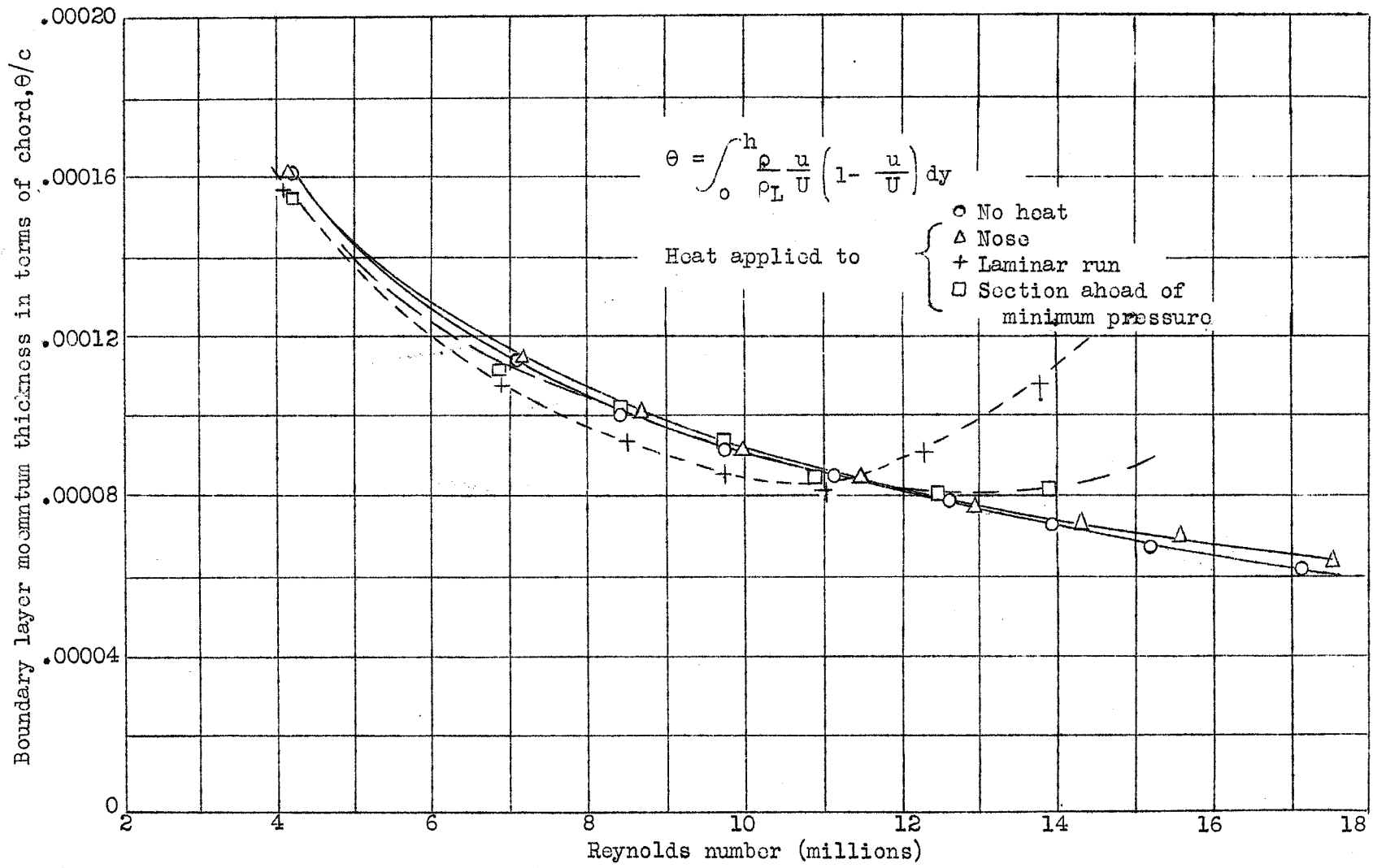


Figure 26.- Boundary-layer momentum-thickness variation with Reynolds number, 29-percent chord. $\alpha = 0^\circ$, $\theta_c = 75^\circ\text{F}$.

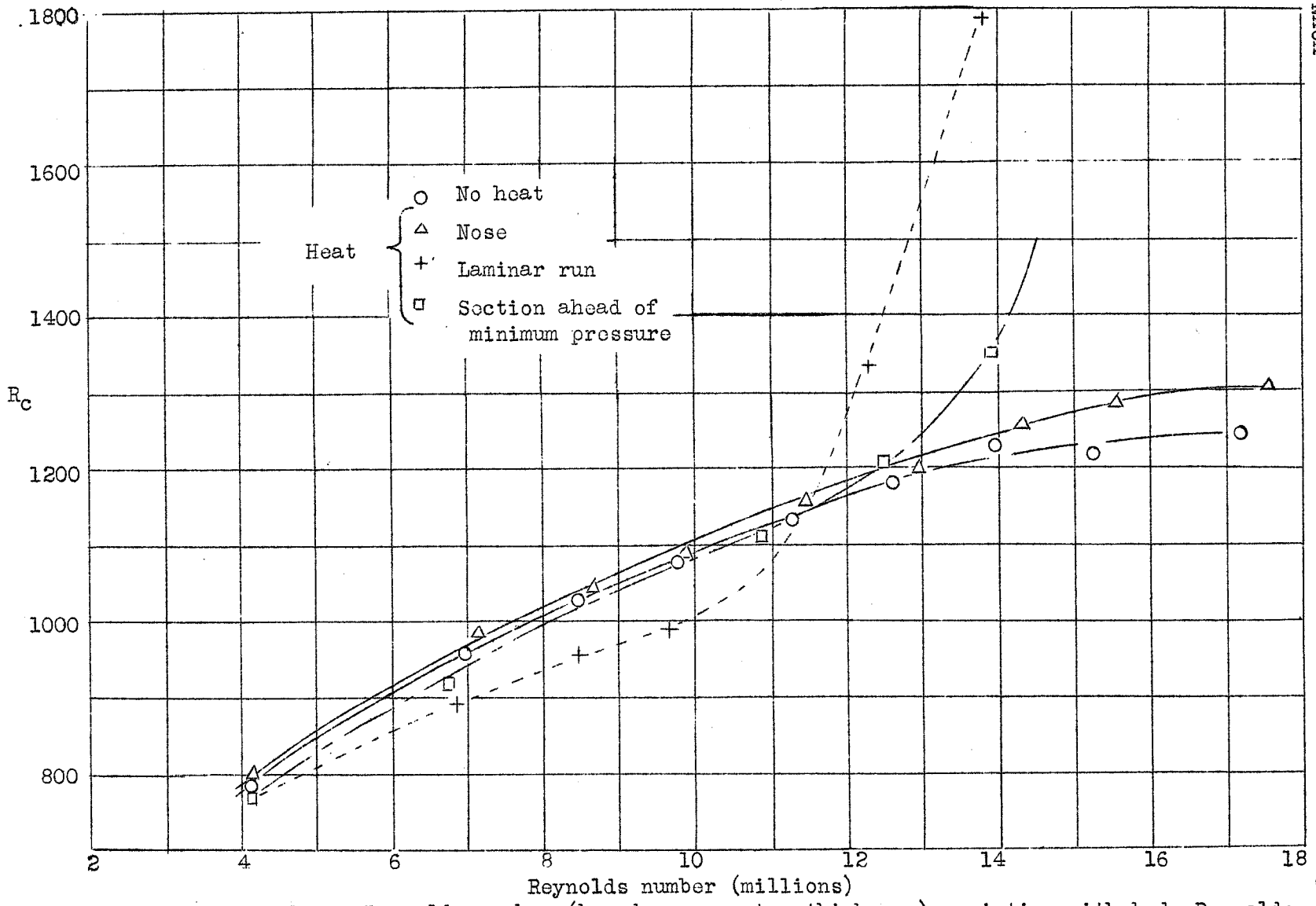


Figure 27.- Boundary-layer Reynolds number (based on momentum thickness) variation with body Reynolds number, 29-percent chord.